Development and Validation of a Synthetic Lumbar Facet Joint and its Load Bearing Characteristics

By Damon E. Mar

Submitted to the graduate degree program in Mechanical Engineering and the Graduate Faculty of the University of Kansas in partial fulfillment of the requirements for the degree of Master of Science.

_____

Dr. Elizabeth Friis – Chairperson

_____

Dr. Sara Wilson – Committee Member

_____

Dr. Carl Luchies – Committee Member

Date Defended: 12/09/2011

The Thesis Committee for Damon E. Mar certifies that

this is the approved version of the following thesis:

Development and Validation of a Synthetic Lumbar Facet Joint and Its Load Bearing Characteristics

_____

Dr. Elizabeth Friis – Chairperson

_____

Dr. Sara Wilson – Committee Member

_____

Dr. Carl Luchies – Committee Member

Date approved: _____

Abstract

There is a substantial need in the spine research community for an anatomical and mechanically correct synthetic model of the human lumbar spine. This model could be used in nearly every aspect of spinal research including the design of implants and the research of new treatments for low back pain. An initial model has already been developed, and the present work focused on the development and validation of the synthetic facet joint in the model. This work was broken down into two primary goals. The first goal was to see if any improvements could be made to the current synthetic facet joint. The second goal was to investigate the load-bearing characteristics of the joint and to see how it compares to human facet joint behavior.

The development of the synthetic facet joint focused primarily on improvements that could be made to the joints non-linear behavior and allow it to be used with currently accepted methods of facet load measurement. Material selection for facet interfaces was directed by considerations of commercial availability and manufacturability. A test protocol was developed which targeted the facet joints ability to provide a transition from neutral to extension stiffness while the specimen underwent axial rotation. The study compared six different interfaces against each other and across multiple test beds. It was found that no single interface showed any significant improvements over the current joint.

The investigation into the load-bearing characteristics of the synthetic facet joint utilized pressure sensitive sensors that were previously identified as the most widely accepted and used method of facet load measurement. A test procedure was designed to show the load-bearing characteristics of the synthetic facet and human facets at fixed applied moment intervals. A secondary procedure was also included to investigate changes in specimen behavior that were induced by the use of the pressure sensors which required an incision to be made in the capsular ligament of each facet joint. It was found that the synthetic facet joint exhibits similar behavior to the human facet joint however it is not statistically similar. It was also found that the cutting of the capsular ligament and insertion of the sensor had a minimal effect on specimen stiffness.

Future work on the synthetic facet joint should focus on the effect which facet geometry has on the overall performance of the facet joint and on improved methods of facet load measurement.

Acknowledgements

I would like to extend my sincerest gratitude to the following for their support during my time as a graduate student.

- Dr. Lisa Friis for her guidance, wisdom, support, and patience over the past two years. She pushed me to succeed and helped me realize the importance and significance of applying my abilities to serve the greater good.
- Dr. Sara Wilson and Dr. Carl Luchies for serving on my graduate advisory committee. I am truly grateful for their contribution of time and assistance in helping me with my work.
- John James and Amy Johnson at Pacific Research Laboratories for their hard work and continual support during the development of the analogue spine model. The spine research community stands to gain an invaluable tool from your efforts.
- The University of Kansas Department of Mechanical Engineering faculty and staff. They have prepared me to be successful in solving any engineering problem and have given me to confidence to go out into the world and make it a better place for all.
- John Domann, Erin Lewis, Brian Good, Nikki Johnson, Nick Tobaben, and Mark Pacey along with all of my other fellow researchers and friends. Their support, perspectives, and continual distractions helped me get through each and every day. My fond memories of our experiences in the lab together will be with me forever.
- My parents Gene Wee and Deloris Boeck for their love, support, and guidance. They taught me to strive to be the best that I can and to pursue a life of satisfaction and happiness.

This work was supported in part by NIH SBIR Grant 5R44 AR054289-02 and Pacific Research Laboratories, Inc.

Contents

List of Figures

List of Tables

List of Abbreviations

AF – Annulus Fibrosis
ALD – Adjacent Level Degeneration
ALL – Anterior Longitudinal Ligament
ASM – Analogue Spine Model
CL – Capsular Ligament
DD – Disc Degeneration
EZ – Extension Zone
FSU – Functional Spinal Unit
ISL – Inter-Spinous Ligament
IVD – Inter-Vertebral Disc
KU – University of Kansas
LF – Ligamentum Flavum
MTS – Material Test System
NP – Nucleus Pulposis
NZ – Neutral Zone
PLL – Posterior Longitudinal Ligament
PRL – Pacific Research Laboratories
ROM – Range Of Motion

SBL – Spine Biomechanics Laboratory
SSL – Supra-Spinous Ligament
TL – Transverse Ligament
TZ – Transition Zone

1. Introduction and Significance

This thesis presents research that was conducted for the development and validation of the facet joint in the analogue synthetic model (ASM) developed by Pacific Research Laboratories (PRL) and the Spine Biomechanics Lab (SBL) at the University of Kansas (KU). This document is organized into four main chapters: 1. Introduction and Significance, 2. Analogue Facet Joint Development, 3. Facet Load Transfer, and 4. Conclusions and Future Work. Chapters 2 and 3 are intended to stand on their own as documents that can be published in a peer reviewed journal. This was done with the intension of making the findings from this work more available to a larger audience than there would be otherwise. As such portions of the background on human spine and facet joint anatomy are repeated in Chapters 1, 2, and 3.

1.1. Low Back Pain

1.1.1. Significance of LBP

Multiple sources report that 75-80% of all people will experience LBP at some point in their life[1-2]. LBP is second only to upper respiratory problems as the primary reason for physician visits [1]. LBP is also the most common cause of work related injuries and is a major contributor to individuals missing work [1]. Of those afflicted with LBP, many require surgery for treatment. In 2004 there were more spinal fusion surgeries performed than the number of hip and knee surgeries combine [3]. LBP cases are on the rise globally, and only shows signs of becoming more and more common [4].

Given the high numbers of cases of LBP, it comes as no surprise that the costs associated with treating it are high. In 2005, it was estimated that more than $85 billion was spent on spine related treatments [5]. Treatment costs continue to rise and it is becoming clear that actions need to be taken to help reduce further cost inflations while reducing the pain and suffering of individuals with LBP.

1.1.2. Causes of LBP

Although the overall causes of LBP are not well understood, many studies have identified common sources that are believed to contribute to LBP. These sources include the following:

- Disc Degeneration (DD) [2].

- Disc herniation which leads to joint instability [2].
- Facet joint instability [6].
- Spinal stenosis [1-2].
- Cardiovascular illness [7].
- Smoking and high cholesterol have been shown to correlate with atherosclerosis [7] and disc herniation [8].
- Vertebral osteophytes [9].

1.1.3. Facet Joint and LBP

It is believed that issues with the facet joint may attribute to LBP. Up to 45% of all LBP cases can be attributed to facet joint related issues [10]. Facet joint pain is typically attributed to issues with the medial branches of the posterior (dorsal) rami of the spinal nerves [10-11]. These nerves carry motor and sensory information to and from the skin and muscles and innervate adjacent facet joints [12].

The clinical significance of facet joint pain and its relation to LBP is a controversial topic due to many reasons including methodological flaws, lack of research, and lack of controlled studies [13]. This indicates that work needs to be done to improve the availability and quality of data from facet joint research. In particular, there is a clear need for the development of a standardize test methodology by which facet joint research can be conducted and compared.

1.1.4. Treatment of LBP

Due to the fact that the causes of LBP are not well known, the methods of treatment are quite varied. There are several non-surgical treatments which have been shown to reduce LBP. A majority of these treatments focus around exercises, stretching, supplements, and pharmaceutical drugs. Although these methods have been proven to be effective, many cases require surgical intervention. Several of these surgical procedures are briefly described below.

- Spinal Fusion: This procedure aims at restoring correct vertebrae spacing, alignment, and stability by rigidly fixing (or fusing) adjacent vertebrae. Fusion hardware typically includes pedicle screws, fusion cages, or other types of spacers. This procedure is commonly used to alleviate LBP cause by vertebral fractures, deformities, and DD. Although spinal fusion has been widely used for years, it has a

high risk of failure. Turner et al. report failure rates as high as 14% [14]. One of the biggest issues related to spinal fusions is adjacent level degeneration (ALD), where segments above and below the fused region degenerate as a result in the change or increase in stress and strain caused by the fusion. ALD is reported to occur in up to 34% of lumbar fusions [15].

- IVD Replacement: This procedure is a common alternative to spinal fusion. This procedure includes the removal of a damaged IVD and the installation of an artificial IVD. This method targets many of the same goals as spinal fusion, although it allows for more motion. With regards to LBP, this procedure relies on the assumption that the pain is derived from the soft tissues of the IVD. This assumption may not be completely valid as pain is often reported to persist even after the procedure is performed [16].
- Laminotomy/Laminectomy: These procedures aim to reduce pressure on spinal nerves and the spinal cord by the removal vertebral lamina. These procedures are commonly used to alleviate LBP caused by ankylosing spondylitis, DD, herniated discs, sciatica, spinal stenosis, and sponylosis. These methods can have high levels of success while imposing minimal effect on spine biomechanics, however long term failure rates (>5 years) can be as high as 25% [17].
- Kyphoplasty/Vertebroplasty: The procedures aim to restore damaged vertebrae by either injecting bone cement (vertebroplasty) or inserting an inflatable balloon (kyphoplasty) into the damaged body to restore is shape and structure. These procedures are commonly used to address LBP associated with osteoporosis and vertebral fractures. Both of these procedures have relatively short surgical times, and little to no healing time. However, these treatments only address symptoms and do not address the causes (primarily osteoporosis).
- Facet Joint Injection: This procedure aim to reduce the sensitivity of nerves from the posterior rami which run into the facet joints by injecting a local anesthesia. This procedure has been widely used for years as a means of managing LBP [18]. However, the long term results of facet joint injects have been shown to not eliminate LBP or its reoccurrence, and additionally, studies have shown that the procedure is a non-specific method of treatment for LBP [19].

1.2. Spinal Anatomy

It is necessary to be familiar with spinal anatomy before reviewing the work presented in this thesis.

1.2.1. Overview of Human Spine

The human spine is the most complicated skeletal structure found in the human body and has four primary functions which are as follows [20]:

- Protect the spinal cord
- Provide support for the head, neck, and upper extremities
- Transfer loads from the head, neck, and upper extremities to the pelvis
- Allow motion of the head, neck, and upper extremities

The human spine is organized into four main sections: the cervical, thoracic, lumbar, and sacral sections as shown in Figure 1.

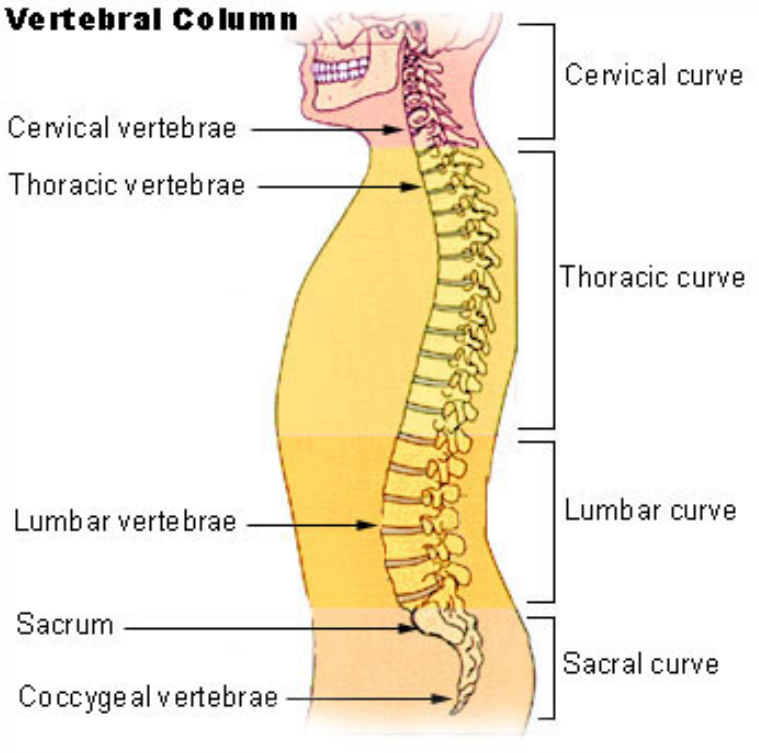

Figure 1: Overview of human spine [21].

Each section is comprised of a series of vertically stacked vertebral bodies (vertebrae) separated by compliant inter-vertebral discs (IVDs). There are typically seven cervical, twelve thoracic, and five vertebrae. The sacral region of the spine is comprised of a set of complex fused bones that form the sacrum (5 bones) and the coccyx (3 bones). When viewed in the coronal plane, the full spine appears as a straight structure with no deviation laterally. When viewed in the sagittal plane, the full spine appears as a structure with four main portions of curvature. The cervical and lumbar sections exhibit lordotic (concave) curvature while the thoracic and sacral regions exhibit kyphotic (convex) curvature. These curves help to provide resistance and elasticity during load transfer through the spine.

1.2.2. Lumbar Spine

The lumbar spine, as previously mentioned, is comprised of five vertebrae. This region of the spine sees the highest forces and moments of the three regions and as such, has the largest and strongest vertebral bodies [22-23]. The size of each lumbar vertebrae increases caudally from L1 to L5 to provide a stable base to support the high loads. The lumbar spine sees a larger range of motion than the thoracic spine since it lacks the addition of rib cage support however its motion is less than that of the cervical spine. Due to the high loads and large range of motion, the lumbar spine is the most common spine region associated with back pain.

Under mechanical loading, both the full lumbar and functional spinal unit (FSU) exhibit a non-linear sigmoid behavior. Hysteretic behavior is seen as a result of the viscoelastic properties of the ligaments and IVD. An idealized mechanical behavior is shown in Figure 2.

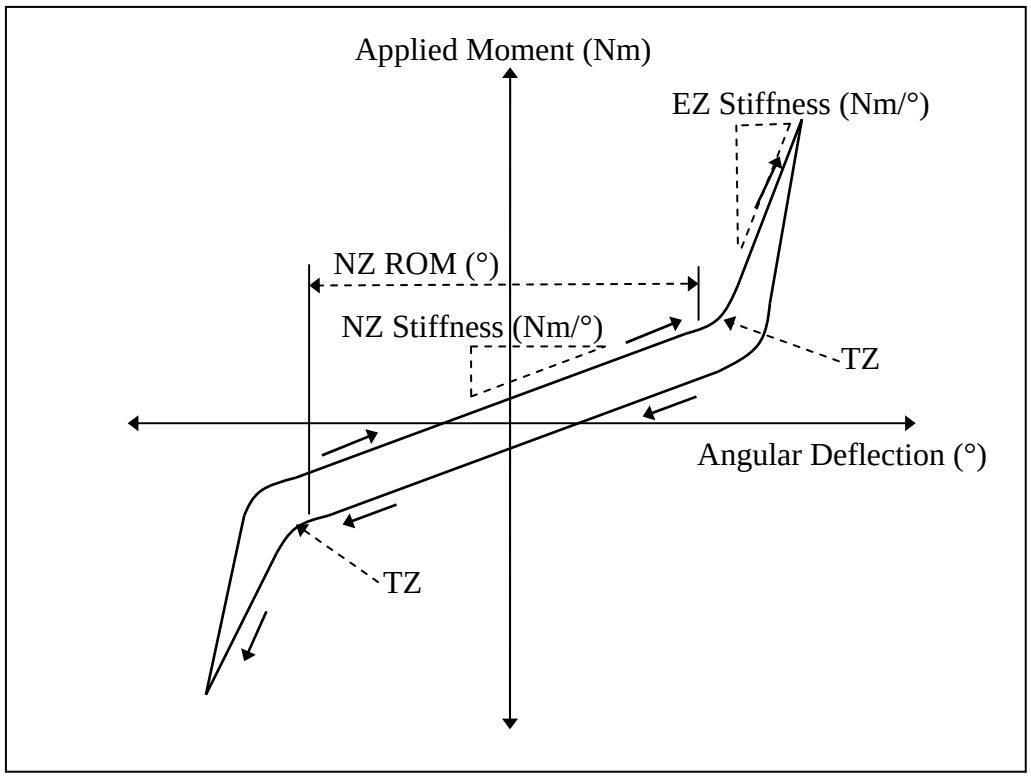

Figure 2: Idealized mechanical behavior of the human spine. The loading direction is indicated by the short arrows. Highlighted elements include neutral zone (NZ) and extension zone (EZ) stiffness, the transition zones (TZs), and the NZ range of motion.

At low angles of deflection, there is a low stiffness region defined as the neutral zone (NZ). In this region, large angular deflections result in relatively small increases in applied moment. This NZ stiffness plays a critical role in the stability of the spine. At higher angles of deflection, a higher stiffness region is produced that is called the extension zone (EZ). In this region, small angular deflections result in relatively large increases in applied moment. The region in which the stiffness transitions from NZ to EZ is referred to as the transition zone (TZ). The full loading angular deflection from the beginning of one TZ to the other is defined at the NZ range of motion (ROM). An example of the mechanical behavior of a typical human FSU specimen is given in Figure 3.

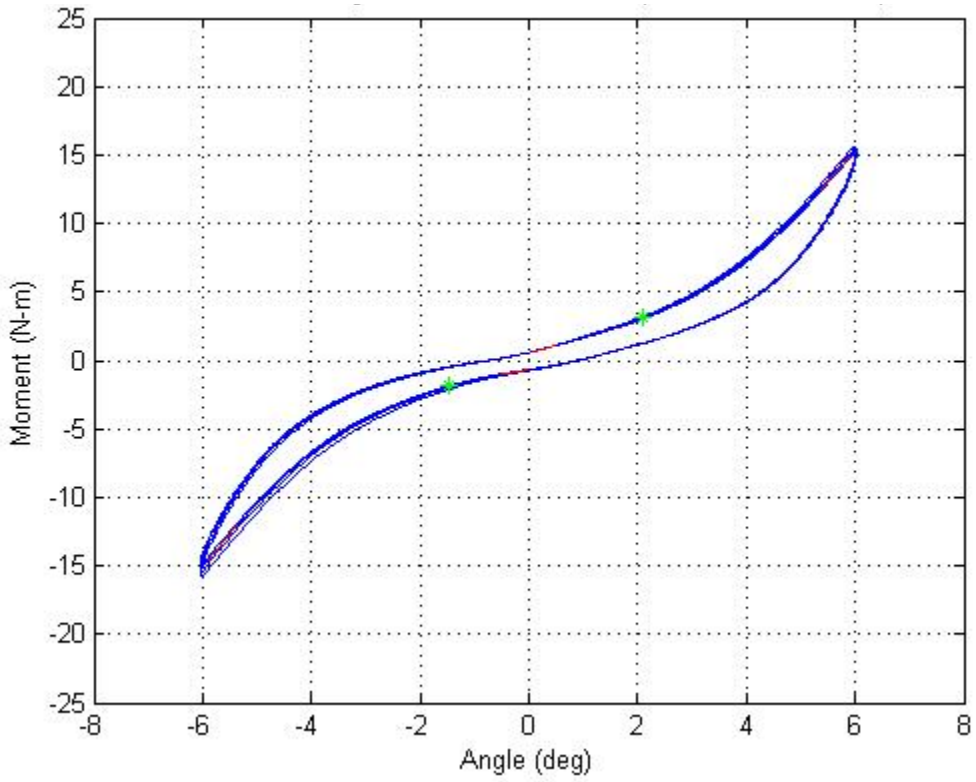

Figure 3: Example of typical mechanical behavior of a human functional spine unit. The neutral zone range of motion is identified by the green stars.

1.2.3. Vertebral Body

The vertebral body acts as the primary load bearing hard tissue in the spine and provides attachment points for ligaments and muscles [24]. All vertebral bodies in the human spine share the same basic elements except for the first two cervical vertebrae. As with most other bones in the human body, the vertebrae is made up of a tough yet thin outer shell of cortical bone and a softer, less dense center of cancellous (or trabecular) bone. The geometry of the vertebral body can be broken down into two main regions: the main body known as the centrum and the posterior ring of processes known as the neural arch. The centrum serves as the primary support for compressive loads transferred through the spine. The neural arch is connected to the centrum by two pedicles (posterior aspects). The neural arch is the primary structure in the spine that forms the spinal canal and protects the spinal cord. There are three types of processes that branch off of the neural arch which are described below.

- Articular Processes: Four articular processes protrude from the pedicles (two superior and two inferior). As mentioned previously, superior and inferior articular processes of adjacent vertebrae make up the facet joints in the spine.
- Transverse Processes: Two transverse processes protrude laterally from each pedicle. These processes provide a means of attachment for the transverse ligaments (TL) and lateral bending muscles.
- Spinous Process: A single spinous process protrudes posteriorly from the neural arch. This process provides a means of attachment for the inter-spinous and supra-spinous ligaments (ISL and SSL respectively).

The primary features of the vertebral body discussed above are shown in Figure 4.

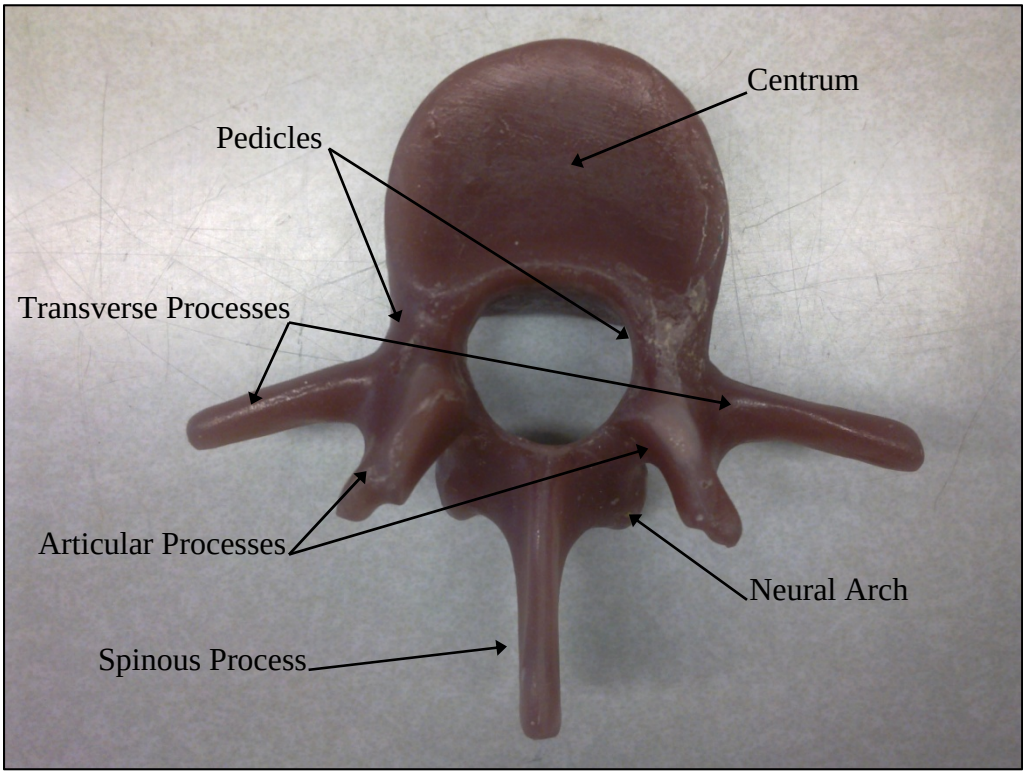

Figure 4: Overview of primary features of a vertebral body. The component shown is a synthetic vertebral body from the analogue spine model.

1.2.4. Spinal Ligaments

Ligaments are mechanical, uniaxial structures which act in tension. In the human spine, ligaments act as primary elements in providing passive stability and resistance to localized motion. There are seven ligaments in the human spine which include the capsular ligaments

(CL), transverse ligaments (TL), inter-spinous ligament (ISL), supra-spinous ligament (SSL), ligamentum flavum (LF), anterior longitudinal ligament (ALL), and posterior longitudinal ligament (PLL). A brief description of each of these ligaments is given below.

- Capsular Ligaments: The CLs connect the facet joints of adjacent levels and encapsulate the synovial fluid within each joint. The fibers of CLs run perpendicular to the line of action of the facets to prevent extreme distraction [25]. The CLs also provide stability in flexion and torsion [26].
- Transverse Ligaments: The TLs connect the transverse processes of adjacent levels and provide stability during lateral motion.
- Inter-Spinous Ligament: The ISL is a thin membrane that attaches adjacent spinous processes. It is believed that the ISL contributes little to the overall stability of adult spines.
- Supra-Spinous Ligament: The SSL, like the ISL, attaches adjacent spinous processes. It is believed that the SSL serves primarily as a cushioning member to the posterior portion of the spine rather than mechanical resistance. The SSL makes up an integrated structure with the ISL.
- Ligamentum Flavum: The LF runs down the posterior wall of the spinal canal and attaches to the neural arch of adjacent levels of vertebrae. The LF primarily provides stability in flexion and lateral bending.
- Posterior Longitudinal Ligament: The PLL runs along the anterior wall of the spinal canal (opposite the LF) and connects the posterior wall of adjacent IVDs. The PLL is not rigidly attached to the vertebral bodies. The PLL primarily serves to resist flexion bending and IVD bulging.
- Anterior Longitudinal Ligament: The ALL runs along the anterior surface of the spine and connects adjacent IVDs similarly to the PLL. Like the PLL, the ALL is not rigidly attached to the vertebral bodies. The ALL serves primarily to resist extension bending and IVD bulging.

1.2.5. Intervertebral Disc

Each pair of adjacent vertebrae are separated by an intervertebral disc (IVD) which forms an amphiarthrodial articulating joint. The IVD acts as a cushion and shock absorber as loads are

transferred through the spine and provides for mobility [27]. The IVD is comprised of two primary parts: an outer ring of tough, fiber-like material called the annulus fibrosis (AF) and a soft, gel-like inner member called the nucleus pulposis (NP). The AF and NP are discussed in further detail below.

- The AF is comprised of a series of concentric lamellae rings of collagen fibers. The orientation of these fibers alternates by 30° across each layer.
- The NP is located at the center of and is contained by the AF. As load is applied to a vertebral joint, hydrostatic pressure is developed in the NP. This pressure is constrained by the AF as hoop stress that is distributed through its layers.

The primary features of the IVD discussed above are shown in Figure 5.

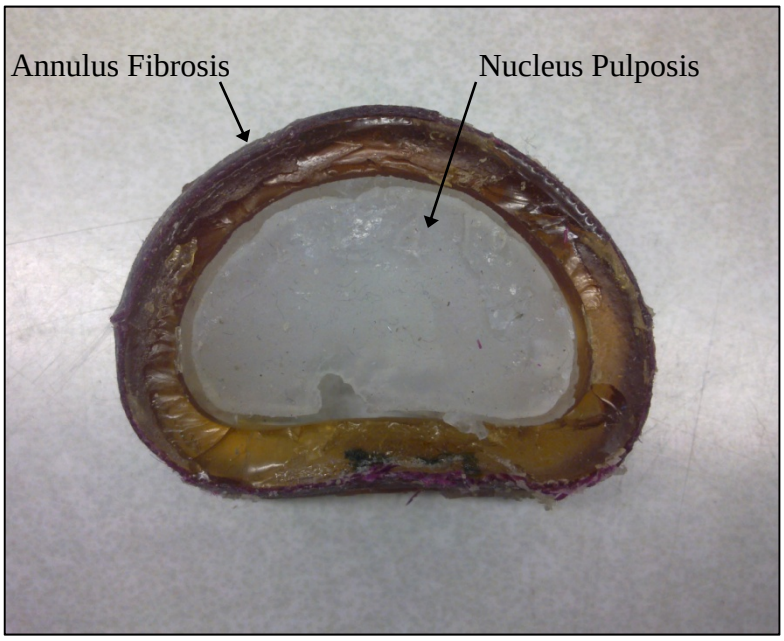

Figure 5: Overview of primary features of an intervertebral disc (IVD). The components shown are synthetic parts from the analogue spine model. In a human IVD, the diving line between the annulus and the nucleus is less defined.

1.2.6. Facet Joint

The facet joint (also known as the zygapophysial or apophyseal joint) is made up of an inferior articular process of one level of vertebrae and the superior articular process of another vertebrae one level below the first. Each vertebrae pair contains two opposing facet joints. A posterior view of a pair of facets is shown in Figure 6.

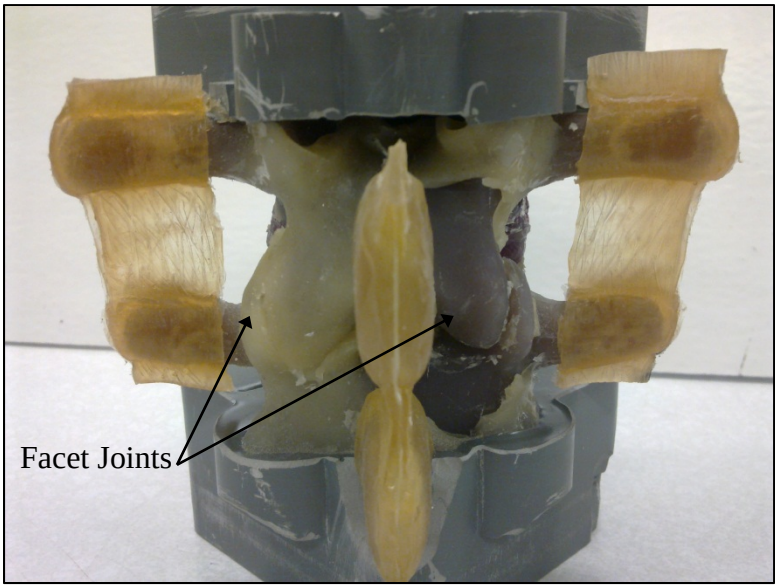

Figure 6: Posterior view of two facet joints. The components shown are synthetic parts from the analogue spine model. The capsular ligament was removed from the right facet to show the articular processes.

The facet joint and the IVD make up the primary load transfer points in the spine. The facet joint provides three main functions within the spine:

- Serves as a means of load transfer between adjacent vertebrae, primarily in bending
- Acts as a shock absorber to dissipate high loads
- Eliminate bone-on-bone contact

In the human body, the interface within each facet joint is made up of articular cartilage on the face of each articular process, synovial fluid between the faces, and the capsular ligament (CL) which encloses the joint (Figure 7).

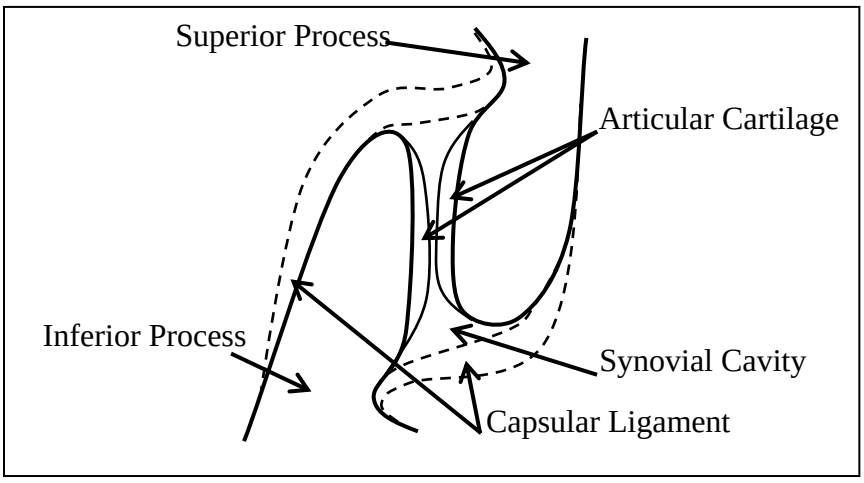

Figure 7: Human facet joint interface.

The cartilage serves as the contact surfaces between the two processes, and the synovial fluid acts as a lubricant to reduce friction during motion. The CLs contains the synovial fluid and hold the joint together.

1.3. Analogue Spine Model

1.3.1. Description and Purpose

The significance of and need for an analogue spine model (ASM) was discussed by Friis et al. [28]. Such a model would have wide spread use in nearly every aspect of spinal research and spinal device design. The following provides brief list of benefits and implications of the ASM.

- Provide a consistent test bed for comparison across tests
- Be used as a means of standardization within the spinal research community
- Eliminate the issues of inconsistency, degradation, and cost associated with cadaver specimen use
- Create availability of spine testing specimens to a wider research community

The funding for the initial development of the soft tissues on the ASM came from an NIH SBIR Phase I grant. This work was done in portions, one focusing on the characterization of the ligaments [29], another on the behavior of the IVD, and another on the behavior of the FSU as a whole [30]. The design of the lumbar ASM was done at the FSU level in order to focus on the characteristics and behavior of a single moving joint rather than the resulting behavior of the

entire lumbar segment. The concept follows that work done at the FSU level designing its mechanical behavior will translate when assembled as a full lumbar ASM segment.

1.3.2. ASM Design and Mechanical Behavior

The ASM includes all of the spinal components presented in the spinal anatomy discussion. The design of the individual ligaments and IVD was researched by LaPierre and Avidano et al. and implemented by PRL [29]. A single FSU of the ASM is comprised of the following:

- Two vertebrae (adjacent levels, L3-L4 for all work done for this thesis) whose geometry was based on samples of human vertebrae. The synthetic vertebrae are made molded of a hardened epoxy and are potted in a nylon base which is used for fixation during testing.
- One IVD composed of an AF and a NP. The synthetic AF is made of a semi-stiff polymer and the NP is a soft, silicon based polymer.
- One of each ligament listed in the spinal ligaments section (CL, TL, LF, ALL, PLL) with the exception that the ISL and SSL are integrated together and are called the SSL. The ligaments are made of various types of molded polymers, some of which have embedded composites to model the non-linear behavior of human ligaments.
- An IVD wrap which was determined to be necessary to achieve proper AF functionality. The wrap was bonded to the vertebral bodies and allowed to slide on the outer edge of the AF.
- Wax is applied to the face of each articular process (before the CLs are molded) to model the synovial fluid that is normally present in human facet joints. The theory and design of the synthetic facet joint is discussed in more detail later.

An example of the typical mechanical behavior of the ASM FSU is shown in Figure 8.

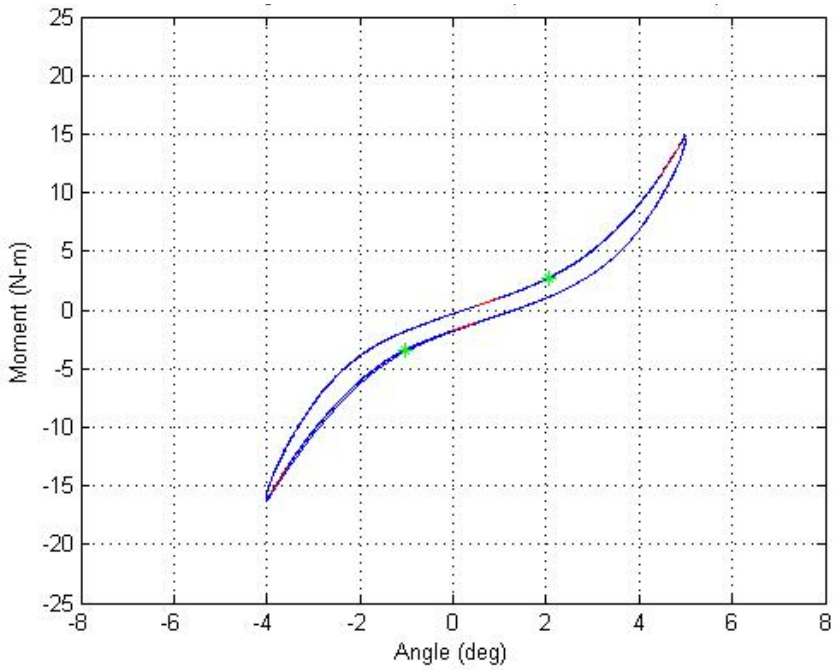

Figure 8: Example of typical mechanical behavior of the analogue spine model. The neutral zone range of motion is identified by the green stars.

The preliminary results from the design of the ASM FSU show that the model behaves in the desired non-linear fashion, however it is too stiff in several modes of bending [30]. Although the current ASM is not in the ideal state, it is acceptable to be used as a test bed for work presented in this thesis as all work presented is done on a relative basis. The work presented in Chapter 2 on the facet interface development focuses only on relative improvements of the TZ of the ASM by comparing six different facet joint interface combinations against each other. The work presented in Chapter 3 represents a first look at the load bearing characteristics of the ASM facet joint and is only intended to identify the current state of the mechanical behavior of the joint.

1.3.3. ASM Facet Joint Improvement Objectives

The underlying goal of the work presented in this section is to continue and finalize the development of the Phase I ASM facet joint and to insure that facet load measurement is possible with currently accepted and utilized technology and techniques. This goal was broken down into two primary research objectives:

1. Investigate potential

2. improvements that can be made to the ASM facet joint which would improve its performance when compared to human facet behavior while considering manufacturability and customer use. The primary improvement to be considered is to address the transition zone between the NZ and EZ during loading. An ideal TZ region should be widely distributed within the NZ and EZ regions and exhibit a smooth, non-linear behavior as seen in human loading behavior.
3. Insure that current facet load measurement techniques can be implemented on the resulting facet joint from the first objective. Additionally, investigate future technologies that could provide improvements in facet load measurement on the ASM.

The work done to meet these two objectives is presented in Chapters 2 and 3 respectively.

2. Analogue Facet Joint Development

Chapter 2 discusses the development of the ASM facet joint. Background on the human lumbar facet joint, previous work on the ASM facet joint, and the study objectives are presented first. The research methods are presented which include a specimen fixture alignment check, interface material selection, and interface material selection. The implications of the results are discussed, and the final interface design is identified.

2.1. Background

2.1.1. Human Lumbar Facet Joint

The facet joint (also known as the zygapophysial or apophyseal joint) is made up of an inferior articular process of one level of vertebrae and the superior articular process of another vertebrae one level below the first. Each vertebrae pair contains two opposing facet joints. A posterior view of a pair of facets is shown in Figure 9.

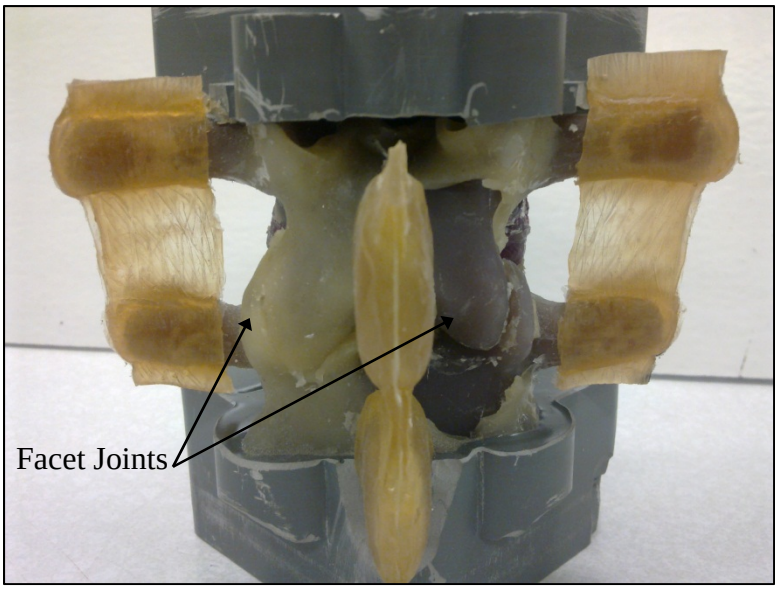

Figure 9: Posterior view of two facet joints. The components shown are synthetic parts from the analogue spine model. The capsular ligament was removed from the right facet to show the articular processes.

The facet joint and the IVD make up the primary load transfer points in the spine. The facet joint provides three main functions within the spine:

- Serves as a means of load transfer between adjacent vertebrae, primarily in bending
- Acts as a shock absorber to dissipate high loads
- Eliminate bone-on-bone contact

In the human body, the interface within each facet joint is made up of articular cartilage on the face of each articular process, synovial fluid between the faces, and the capsular ligament (CL) which encloses the joint as shown in Figure 10.

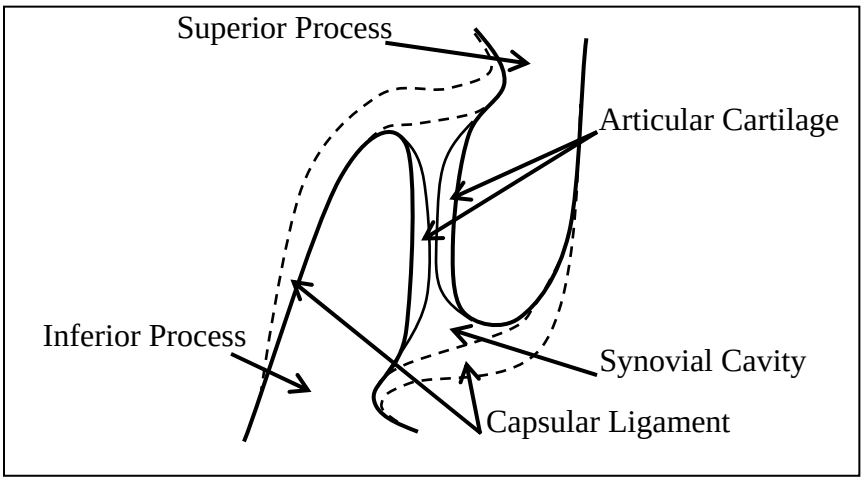

Figure 10: Human facet joint interface. The face of each articular process is coated with a layer of articular cartilage. The synovial cavity is filled with fluid that is contained by the capsular ligament.

The cartilage serves as the contact surfaces between the two processes, and the synovial fluid acts as a lubricant to reduce friction during motion. The CLs contains the synovial fluid and hold the joint together.

2.1.2. Previous work on ASM Facet Joint

Various aspects of the ASM were developed over a number of years which included the characterization and material identification of the vertebrae, IVDs, and ligaments [28, 31]. Additionally, a preliminary facet joint was specified and implemented on the trial FSUs during development. This preliminary facet joint was based on an inverse synovial joint; one in which the modeled fluid was located on the face of the articular processes and the articular cartilage was modeled as a boundary that contained the fluid between the two articular processes that make up the joint (Figure 11).

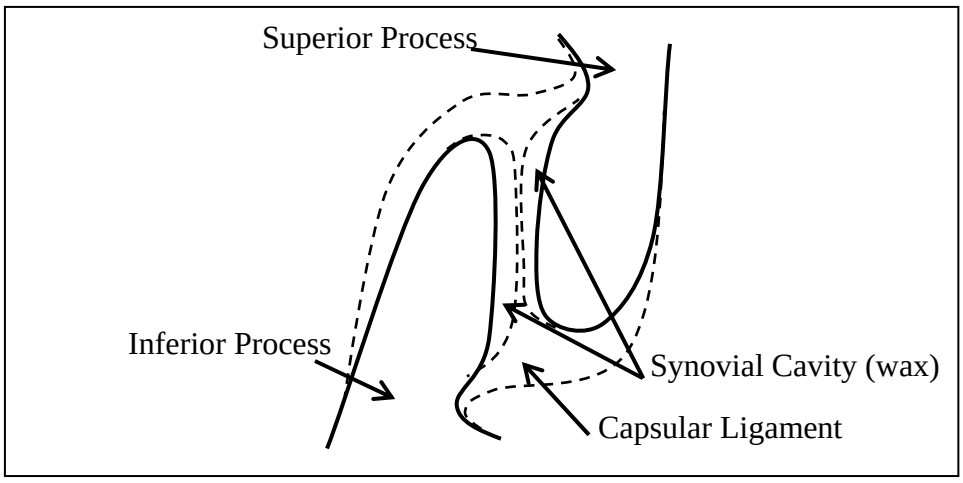

Figure 11: Inverse facet joint interface concept. This interface differs from the human facet joint in that the synovial fluid and articular cartilage are reversed: the fluid is on the facet of each articular process and the cartilage is between them.

In the ASM, the CLs serve as both as the traditional ligament and as the boundary material separating the articular process faces. The synovial fluid was modeled as a thin film of wax which is applied to each process face before molding the CLs. The CLs are molded from a soft and elastic elastomer provided by PRL.

The concept behind the functionality of the inverse synovial joint is that although the order in which the individual layers are reversed, the same mechanical properties are achieved. Rather than the lubrication acting between the two articular surfaces, it acts on the face of each articular process. The portion of the CL that goes between the two lubricated faces acts to dampen the load transfer in the joint, much like the articular cartilage in a human joint does.

2.1.3. Study Objectives

The main purpose of this portion of research was to see if the current ASM facet joint could be improved upon while still maintaining the original ASM design requirements [31]. The improvements were to be evaluated in two main groups: performance and manufacturability. The first group focuses primarily on how well the material, when implemented, develops a smooth, non-linear transition between NZ and EZ motion. The second group focuses on how realistic the material is to work with in a manufacturing setting. Considerations for this group include availability, ease of preparation, and ease of application.

In addition to improving the joint, another goal was to make the joint as compatible with Tekscan pressure sensors (Tekscan Inc., South Boston MA) as possible. Early on in the development of the ASM, these sensors were identified as the most suitable option for facet load measurements among various alternative methods [31]. These alternative methods are discussed in more detail in Chapter 3. Tekscan model 6900 pressure sensors were used for this research as they are the most commonly used type for facet load measurement (Figure 12).

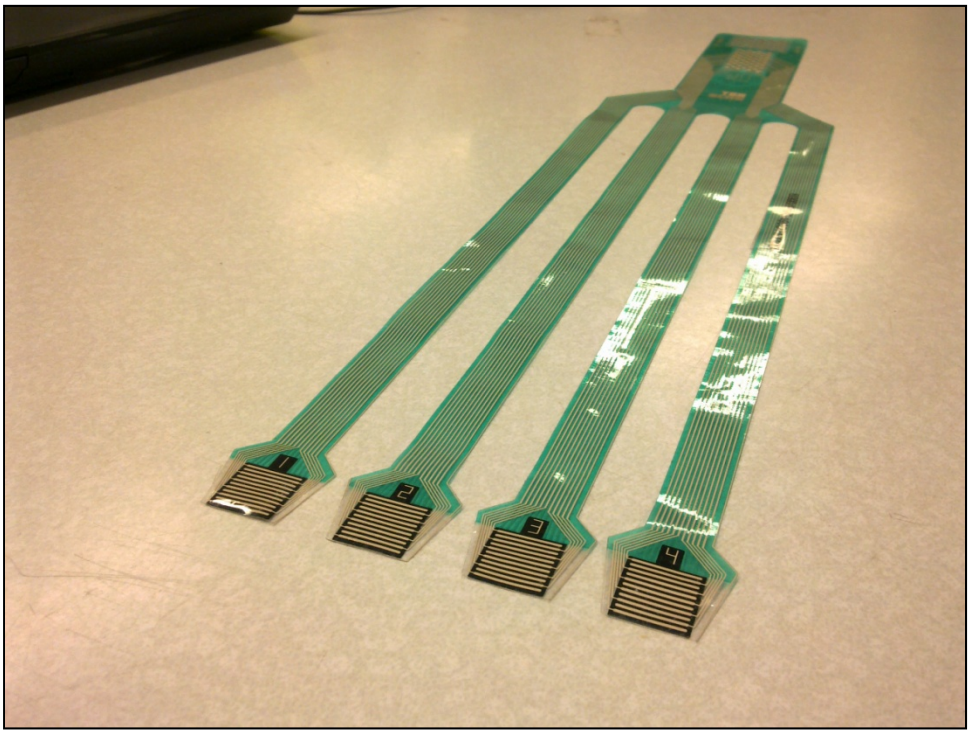

Figure 12: Tekscan model 6900 pressure sensor. Only two of the four sensors are used during each test.

When inserted between two articular processes in a facet joint, the Tekscan sensor can measure contact area, force distribution, and force magnitude. These metrics can provide valuable insight for product development and spine research [32]. The compatibility of the ASM facet joint with the Tekscan sensors was considered a minimum requirement for any interface considered. Adequate compatibility was defined as one in which an incision could be made easily in the CLs with standard laboratory or surgical tools and the Tekscan sensor could easily be slid into the incision so that the active pressure sensing area was centered about the contact area of the facet joints.

The final goal of this study was to investigate the amount of NZ ROM variance that was present in the test set up used for the interface tests. This check would determine the range of possible angular variance for both ideal and non-ideal alignment combinations.

2.2. Methods

Testing was done with a MTS Mini Bionix 858 hydraulic load frame (MTS Systems Co, Eden Prairie MN). The MTS machine used by the University of Kansas (KU) Spine Biomechanics Lab (SLB) is capable of applying three modes of loading: axial tension and compression, axial rotation (torsion), and bending in both the lateral and flexion-extension directions depending on specimen orientation. In each of these modes, the Mini Bionix records load (force and bending moments) and displacement (distance and angle) data for all channels at a sample rate of 100Hz. The specimen is held rigidly at each end (top and bottom) as shown in Figure 13.

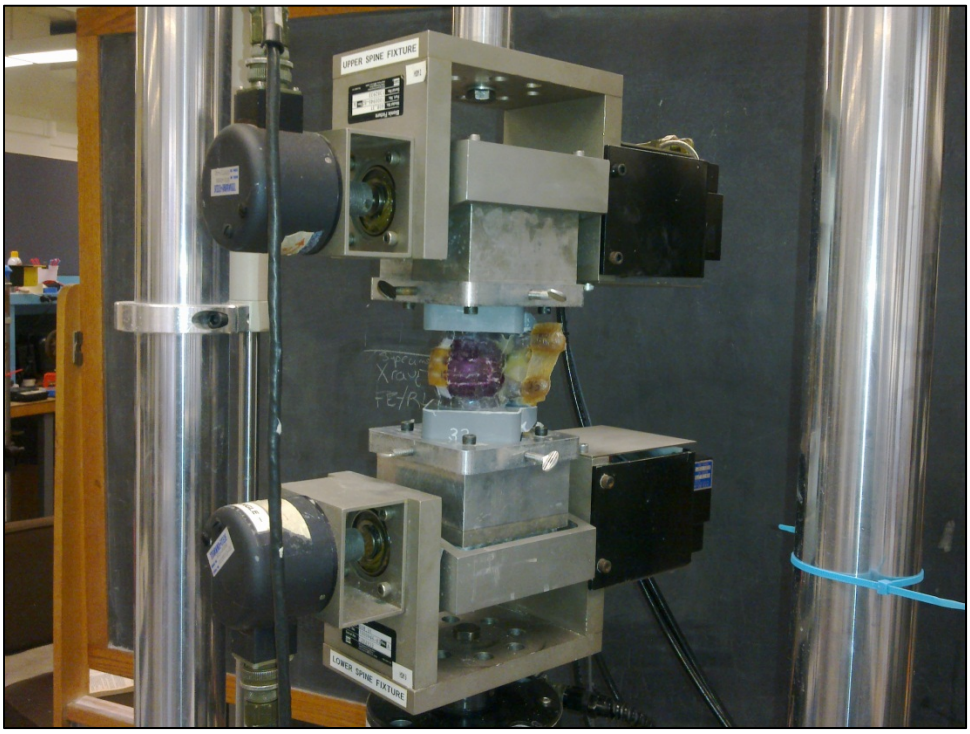

Figure 13: Functional spine unit loaded into MTS hydraulic load frame.

All bending modes, including axial rotation, are performed at a rate of 0.92°/sec. Wilke et al. reports anything between 0.5°/sec and 5°/sec as an acceptable rate that does not affect the results [33].

2.2.1. Interface Material Selection

One of the primary goals in this experiment was to identify a material that could serve to mimic the mechanical functions of synovial fluid; the material was not intended to be an exact synthetic replica. The modeling and development of a true synovial fluid replacement is well beyond the scope of this work. A set of requirements were generated to help simplify the material selection. These requirements are as follows:

- Easily formed or molded to a desired shape
- Common and readily available for purchase in bulk quantities
- Shelf life of at least two years
- Either available as or able to be formed into a thin sheet so it can be die cut
- Able to remain as a solid up to 100°F for shipping concerns

Several materials were identified that could meet these requirements. A basic description and overview of each material is given in Table 1.

Table 1: Materials for facet interface testing.

Material	Description	Intended Mechanical Function
A90	Original wax used in ASM	Synovial fluid
Elastomer A	Polymer used for original ASM CLs	Cartilage
Paraffin	Common wax	Synovial fluid
Beeswax	Common wax	Synovial fluid
Candle Gel	Mineral oil and resin	Synovial fluid and/or cartilage
Petroleum Jelly	Common lubricant	Synovial fluid
Elastomer B	Polymer used by PRL	Cartilage
Wax Emulsifier	Wax additive to reduce stiffness	Synovial fluid enhancement

Each material was chosen to represent a slightly different behavior than the others for its intended use. The A90 and Elastomer A were the original materials specified for the ASM facet joint by the SBL and PRL. Paraffin was chosen as it is one of the most readily available commercial waxes and was found to be relatively stiff and brittle compared to A90. Beeswax was chosen as an alternative to paraffin as it was found to be softer and less stiff than A90. The

candle gel was considered because of its jelly-like composition and its ability to be broken down and move around (to flow) within the enclosed joint. Petroleum jelly was considered as an alternative to the candle gel as it exhibits a slightly more fluid-like behavior. Elastomer B was considered as an alternative cartilage material that would replace the Elastomer A that normally flows between the facet joint during molding. Elastomer B exhibited slightly more compliant behavior than Elastomer A and had a lower surface friction.

The combination of a lubricating material (synovial fluid) with a barrier material (cartilage) makes up an interface for the facet joint. The different combinations of materials form the variables for the interface material tests.

2.2.2. Interface Material Preparation

During the preparation of each specimen, the interface was assembled in a standardized procedure. The synovial fluid material was melted and or rolled out into a thin sheet, approximately 0.0625" thick at most. Once the material was cooled and set, two 0.3125" diameter discs were cut out using a circular die cutter. A corresponding 0.3125" diameter disc of cartilage material was also cut out from sheets produced by PRL. The two synovial fluid discs were applied to the superior and inferior articular process faces by gently pressing them on until they stuck. The cartilage material disc was then pressed onto one of the two synovial material discs. This process was repeated for the other facet joint on each specimen. The process is shown in Figure 14.

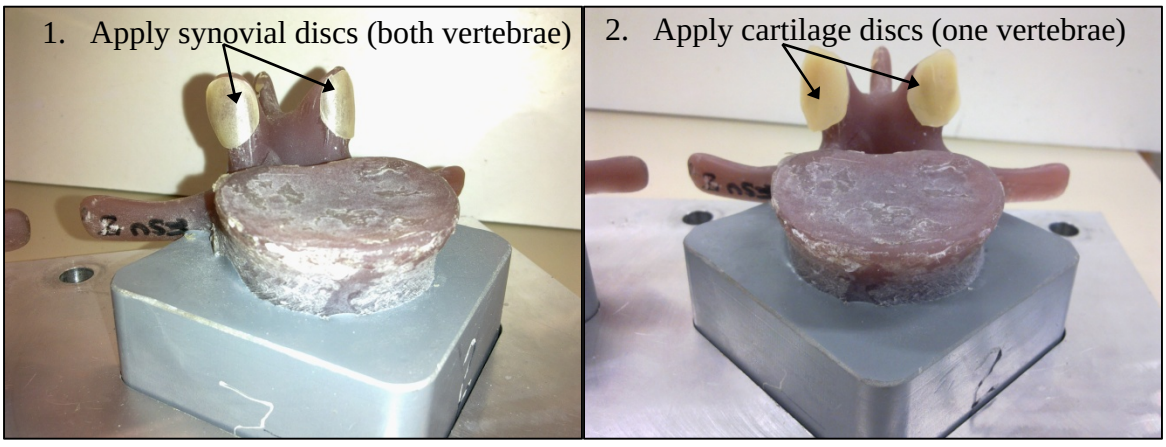

Figure 14: Facet interface assembly process. The first step is to apply synovial discs to the face of each articular process (only the superior pair is shown in the left figure). The second step is to apply the cartilage discs on top of the synovial discs to one vertebra.

Once each interface was prepared, the superior and inferior vertebrae of each specimen were set into an assembly fixture as shown in Figure 15.

Figure 15: Facet interface assembly fixtures with vertebrae pairs.

A semi-rigid IVD was placed between each pair of vertebrae, and then the two halves of the fixture were attached together as shown in Figure 16.

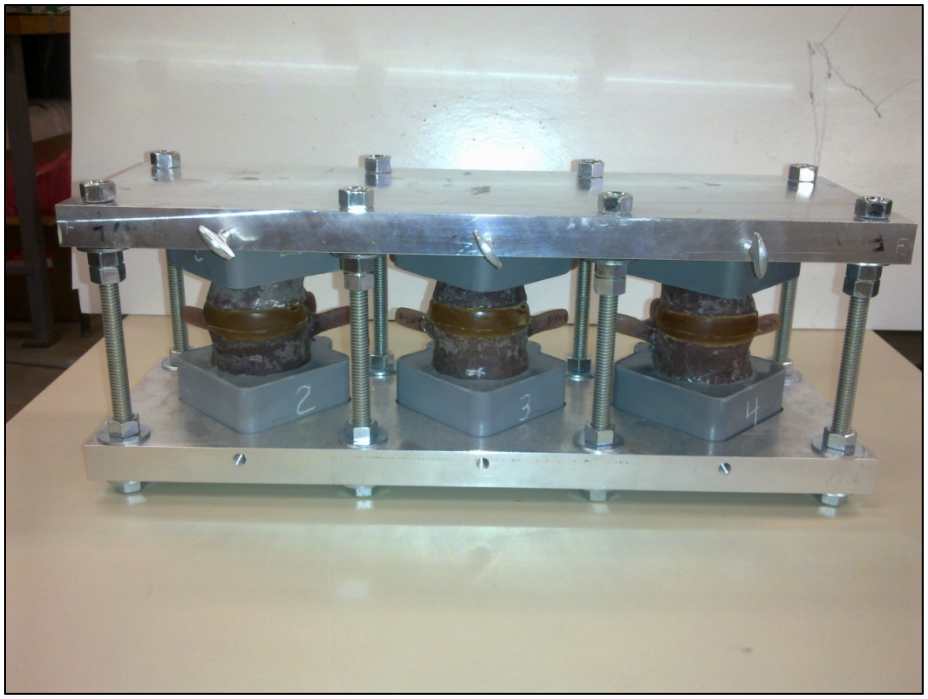

Figure 16: Interface test specimens in fixtures with intervertebral discs.

The vertical spacing between the upper and lower plates of the fixture is set by the nuts and washers on the all-thread rods. The height was set to correspond to an axial compressive preload of approximately 10N. This preload was enough to insure that the specimens were properly seated in the assembly fixture yet minimal enough that it had little effect on neutral alignment of the facet joints. Once the fixtures were tightened down, several layers of Elastomer A, the regular CL material used on the ASM, were applied to each facet joint to encapsulate the interface as shown in Figure 17.

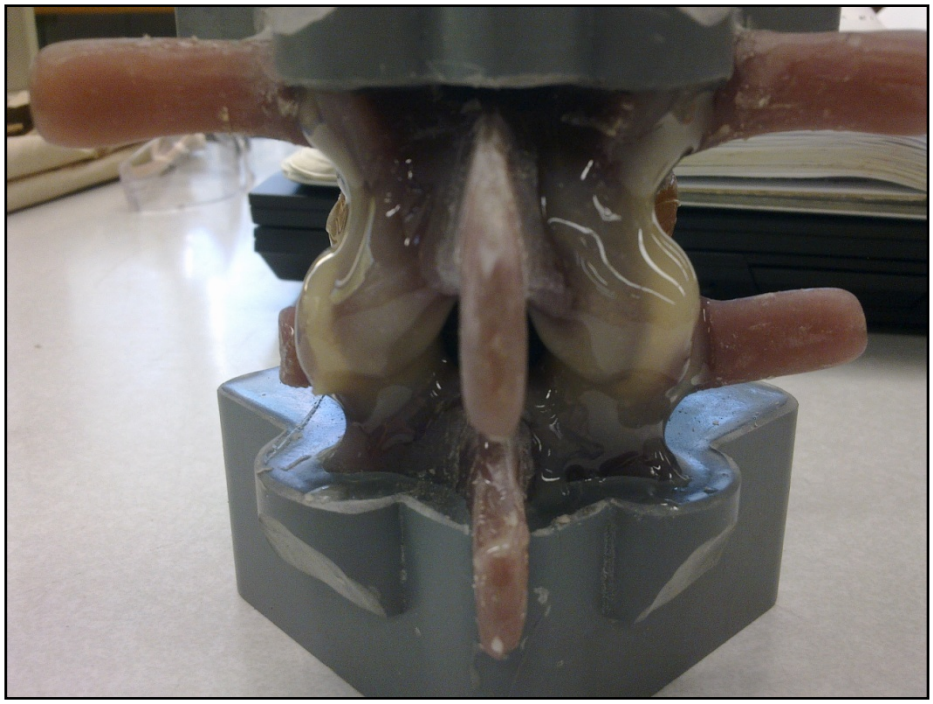

Figure 17: Elastomer A applied to synthetic facet joints.

The prepared facet joints were then allowed to cure for a minimum of 12 hours at room temperature in the assembly fixtures before removing for testing.

2.2.3. Facet Interface Testing

Six vertebrae test pairs were used for the interface testing. The testing was done in three sets. The first set was done with no interface and no CLs to give the baseline behavior for each specimen. This baseline behavior would be used as a reference to see how each interface behaved. After the first set was done, the second set was run which included six different interface combinations utilizing all of the materials considered for this experiment. These combinations were implemented on the six vertebrae test pairs and are listed in Table 2.

Table 2: Table for initial set of interface combinations

Combination	Synovial Fluid	Cartilage
1	Paraffin	Elastomer A
2	A90	Elastomer B
3	Petroleum Jelly	Elastomer A
4	Beeswax	Elastomer A
5	Candle Gel	Candle Gel
6	Paraffin & Emulsifier	Elastomer A

The results from the second set would be analyzed as a comparison of each interface behavior to the specimen's baseline behavior. This would describe how each interface behaved as a transition-inducing mechanism. Once each individual interface's behavior is described, the six initial interfaces would be compared to each other. The top three from this set would be tested again in the third set. For the third set, two vertebrae test pairs of each interface would be tested. This was done to verify the initial performance across multiple vertebrae pairs.

The test procedure for each specimen was broken down into a series of four specimen configurations:

1. Test specimen intact
2. Cut CLs and test
3. Insert lubricated mock sensor and test
4. Remove mock sensor and test

Each specimen was aligned in the same position in the MTS spine jigs for all tests, and the specimen remained fixed in the jigs over the course of all four test steps. The vertical height of the L3 vertebra was set in the same manner that was done for the base alignment check.

2.2.4. Specimen Potting and Alignment Check

Each vertebra in the ASM is potted in a nylon base that serves as the orientation reference for fixing the specimen to the test equipment. The dimensions of these potting bases were designed for a loose fit between the specimen and the fixtures used in the SBL MTS machine for ease of use. The clearance is approximately 0.05" when the base is pushed against a corner of the jig as shown in Figure 18.

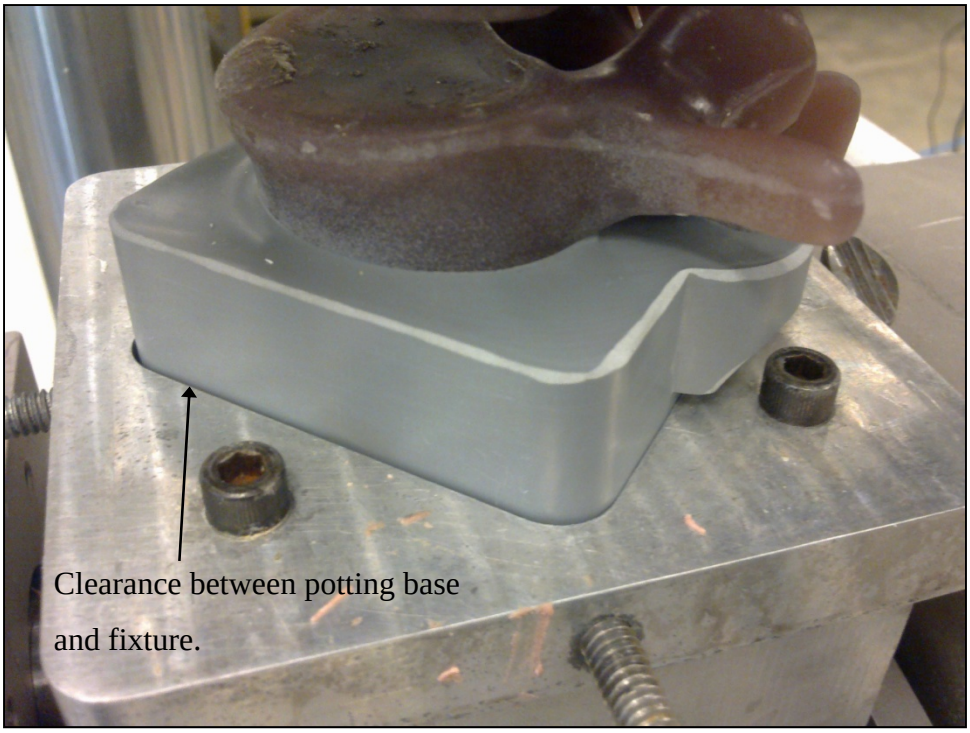

Figure 18: Clearance of specimen potting base and test fixture. Note the gap that is present between the potting block and fixture in the left corner. The same amount of clearance is present in both the upper and lower fixtures on the University of Kansas Spine Biomechanics Laboratory MTS machine.

Since each vertebra is rigidly fixed to a potting base, the alignment of each base in the MTS fixtures contributes directly to the specimens NZ ROM. An experiment was set up to investigate the amount of variance in specimen behavior that could be expected from fixture alignment.

Eight different alignment combinations were considered for the potting bases and are shown in Figure 19.

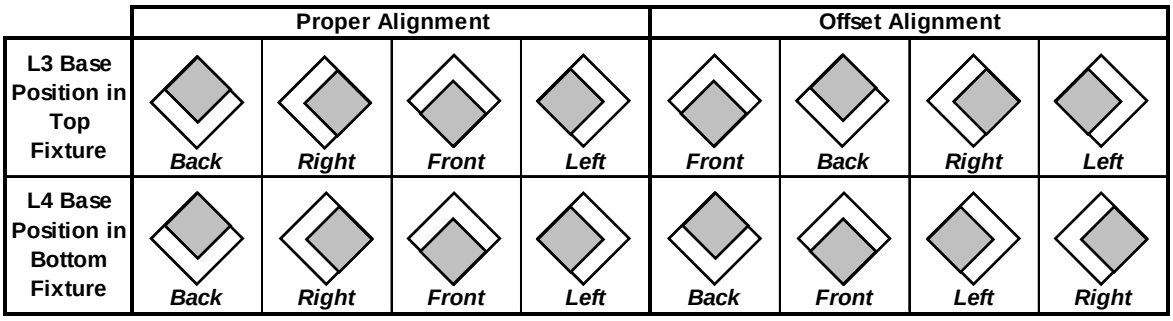

Figure 19: Alignment positions of L3 and L4 potting bases considered for alignment check. The four proper alignment combinations represent realistic alignments. The offset alignment combinations represent worst-case alignments and show the maximum possible misalignment.

The first four alignments were considered to be the positions that should best center the specimen and introduce the least amount of variance. The remaining four alignments were considered worst-case conditions which would show what the worst possible variance could be. For each alignment combination, a single trial was run for each specimen. The vertical spacing of the upper and lower vertebrae was set using an IVD spacer that had the same geometric properties as the one found in the full ASM, but was effectively rigid in stiffness. With the axial rotation angle of the MTS machine set at absolute zero (center), the IVD was placed between the vertebrae and then the upper fixture was lowered down toward the lower fixture until a -10N axial preload was achieved. This amount of preload was used as it was enough to fully seat the vertebrae on the IVD. The axial displacement at which the preload occurred was recorded. The axial preload was then removed by raising the upper fixture, the rigid IVD was removed, and the axial displacement was returned to the position at which the -10N preload occurred. Figure 20 shows a specimen loaded in the MTS jigs with the appropriate positioning.

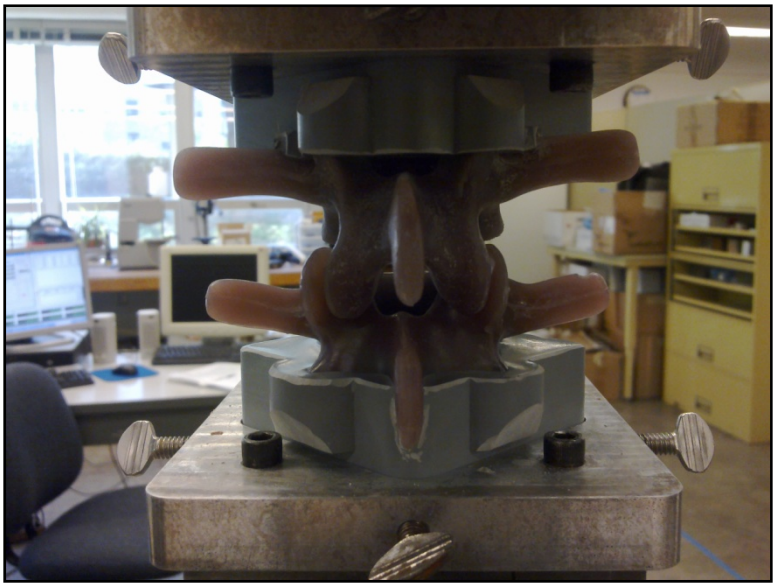

Figure 20: Posterior view of potted vertebrae pair loaded in MTS jigs.

Each specimen then underwent axial rotation in both directions, and the angles at which right and left facet contact initially occurred were recorded.

2.3. Results

2.3.1. Facet Interface Test Results

The results from the facet interface tests are presented in Appendix A. The results are organized into two groups: the first being a comparison between baseline performance and the six initial interfaces and the second being a comparison between the three best from first set compared across two specimens each. An example of a typical result is shown in Figure 21.

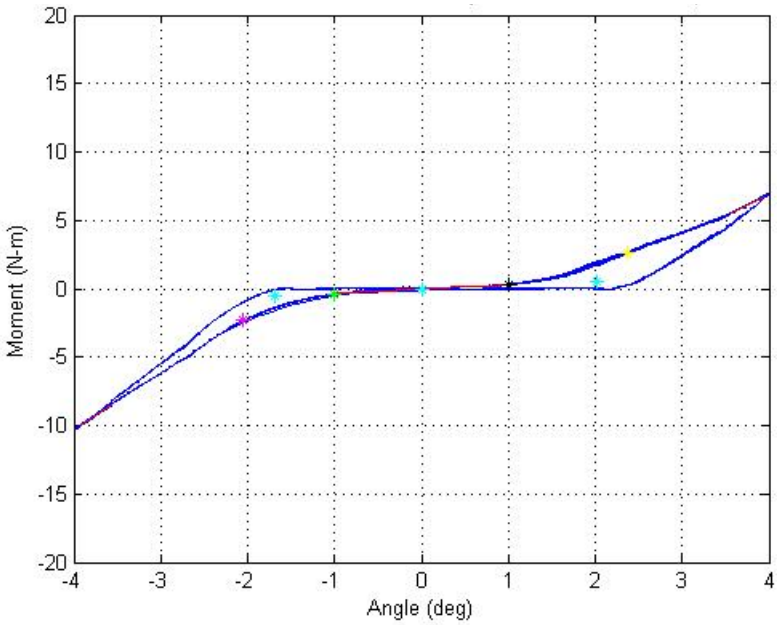

Figure 21: Example of typical interface test results. The star markers on the plot are from the quantitative analysis that define the start (black and green markers) and end (yellow and pink markers) points of the transition region. The light blue markers show the ends of the neutral zone range of motion and its center.

2.3.2. Alignment Results

As was discussed previously, the specimen potting base alignment check was done to determine the amount of variance due to base alignment in the MTS jig fixtures. The angular difference between the right and left facet contact angles is defined as the NZ ROM for this experiment. The values for the proper and offset base alignment positions are presented in Table 3 and Table 4 respectively. Table 3 shows that the position averages are not all the same. Note that there is also variance across the specimen averages as well and that the specimen standard deviations are less than the position standard deviations. In Table 4, it can be seen that both position and specimen standard deviations are higher for the offset case than the proper case. The variance for the raw data sets, the specimen averages, and the position averages are given in Table 5. The variance seen in all three sets of data is higher for the offset case than the proper case.

Table 3: Neutral zone range of motion values from alignment check for proper alignment of bases.

Specimen	Positions: L3 Base/ L4 Base (°)				Specimen Avg.	Specimen Std. Dev.
	Back/Back	Right/Right	Front/Front	Left/Left		
1	3.80	4.02	3.87	3.89	**3.90**	**0.09**
2	2.60	3.19	3.25	3.02	**3.02**	**0.29**
3	3.90	3.98	4.37	4.05	**4.08**	**0.21**
4	4.15	4.34	4.82	4.46	**4.44**	**0.28**
5	3.40	3.94	3.99	3.69	**3.76**	**0.27**
Position Avg.	**3.57**	**3.89**	**4.06**	**3.82**		
Position Std. Dev.	**0.61**	**0.42**	**0.59**	**0.53**		

Table 4: Results from alignment check for offset alignment of bases.

Specimen	Positions: L3 Base/ L4 Base (°)				Specimen Avg.	Specimen Std. Dev.
	Front/Back	Back/Front	Right/Left	Left/Right		
1	3.14	4.38	3.97	3.71	**3.80**	**0.52**
2	0.35	4.04	3.20	2.58	**2.54**	**1.58**
3	2.78	5.04	3.86	4.10	**3.95**	**0.93**
4	2.89	5.48	4.53	4.48	**4.35**	**1.07**
5	2.49	4.48	4.01	3.52	**3.63**	**0.85**
Position Avg.	**2.33**	**4.68**	**3.91**	**3.68**		
Position Std. Dev.	**1.13**	**0.57**	**0.48**	**0.72**		

Table 5: Variance of raw data, specimen averages, and position averages from alignment check data.

Variance (°)	Proper Alignment	Offset Alignment
Raw Data	0.28	1.25
Specimen Avg.	0.28	0.45
Position Avg.	0.04	0.96

It is important to note that the variance presented above is specific to the SBLs test set up only. The variance is directly affected by the specimen potting base and test equipment fixture geometry.

2.4. Discussion

2.4.1. Interface Material Analysis

The analysis of the interface tests was initially done quantitatively with a Matlab code (The Math Works Inc, Natick MA) that was designed to locate the start and end points of the transition region that connects the NZ and EZ regions as shown in Figure 22.

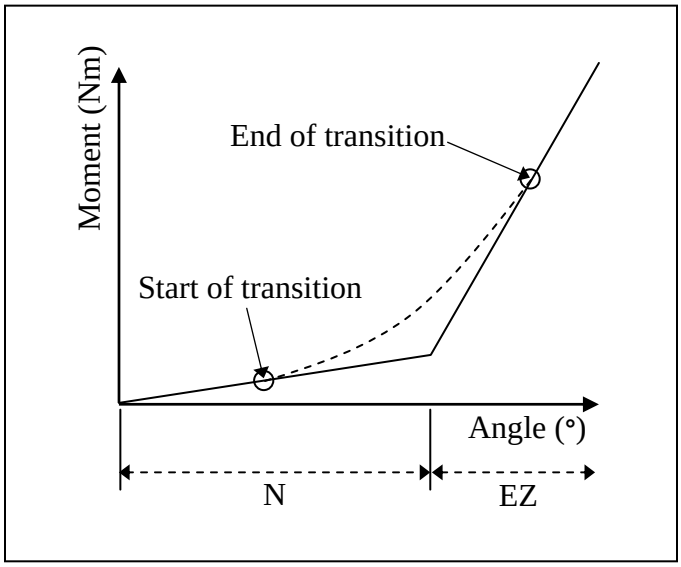

Figure 22: Idealization of transition region between neutral zone (NZ) and extension zone (EZ) stiffness.

The difference between the angles at which these two points occurred was to be used as a metric to describe how well a given interface smoothed out the transition from NZ to EZ stiffness; the greater the difference, the better the transition. These values were normalized to the baseline behavior for the vertebrae pair that each test was conducted on to be able to compare results across the different vertebrae pairs. After the initial set of tests was done and the first set of interface data was analyzed, it was found that there was too much variance across vertebrae pairs and individual tests to be able to make any statistically significant comparisons. In light of this, the evaluation of the interface testing was done on a qualitative basis. The hard points defined by the analysis program were translated to qualitative guidelines that would be used by a human observer to perform the comparisons. These guidelines were as follows:

- ***Interface shows a clear change in appearance of a transition region compared to its respective baseline behavior.*** A clear change was defined as one that could easily be differentiated from the baseline behavior. It is important to note that this guideline

was only applied to inter-specimen comparison only; this guideline was not used to compare across different interface combinations. An example of an interface meeting this guideline is provided in Figure 23.

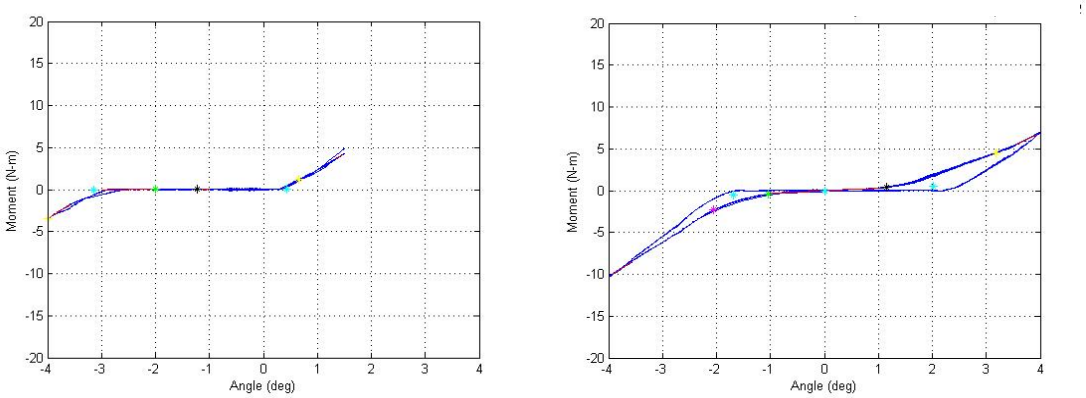

Figure 23: Example of a clear change in appearance of a transition region compared to a baseline behavior.

- ***Interface shows a well-developed, non-linear transition region which has beginning and end points that are a large distance apart.*** A large distance between these points was defined as one where the beginning point occurs roughly at least half way into the baselines NZ region and extends for roughly the same length into the EZ region. The guideline was compared both within tests done on each specimen and across different interface combinations. Examples of a baseline comparison and an interface comparison are shown in Figure 24 and Figure 25 respectively.

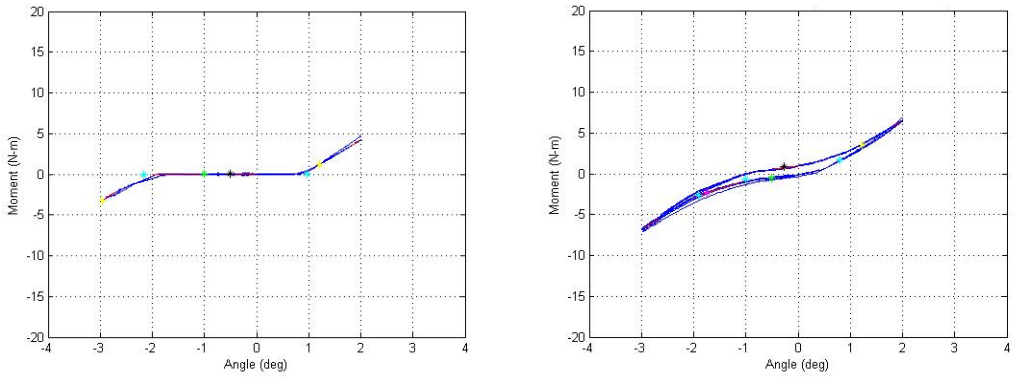

Figure 24: Example of a large distance between start and end points of a transition region compared to a baseline behavior.

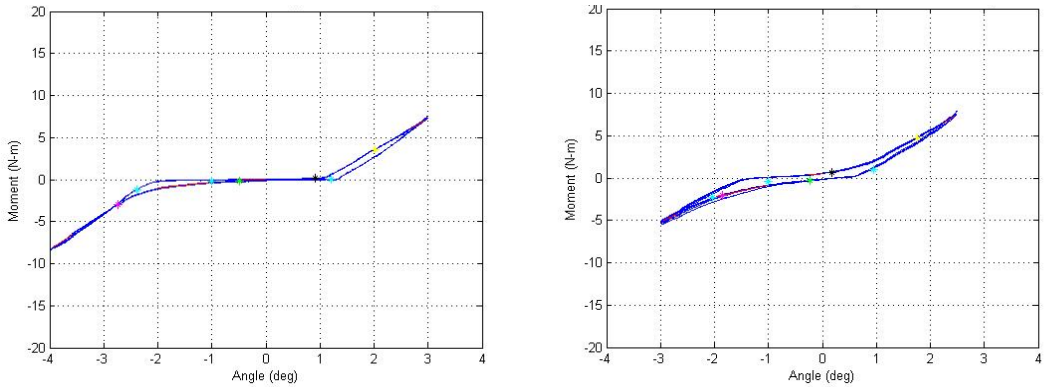

Figure 25: Example of a large difference in distance between start and end point of a transition region between two different interface combinations. The interface in the right image shows a much better distance between start and end points than the interface in the left image.

The guidelines described above were presented to five human observers that were included in the qualitative study. Each observer first identified the specimens that they felt met the first guideline (clear development of TZ). They were told to choose at least three interfaces. Next, the observer was told to look at three interfaces which were shown on two different test pairs and to try and rank the three from best to worst based on how well each met the two guidelines presented. The results from this method revealed that of the top three interfaces identified as ones which met the qualitative guidelines, no single one performed any better than the others.

It is important to note that this facet interface investigation was done with only the CLs and interface materials. In the actual ASM, the facet joints work in conjunction with the other ligaments and IVD. The analysis of the results from this testing was done purely on a relative basis; the actual specimen behavior is derived from all the FSU components as a whole. The focus of this work was on the transition zone between NZ and EZ only. NZ and EZ stiffness were not included as variables as the test specimens used in this testing were not fully functional FSUs.

2.4.2. Impact of Specimen Alignment

The specimen base alignment check was done to provide insight into the amount of variance due to base alignment that could be expected for any test performed with a given vertebrae test pair while using the MTS machine in the SBL. In general the actual variance will normally be

much closer to the lower end of the range as the high values are the worst possible cases and are easily avoided with proper attention while loading a specimen in the MTS fixtures. Ultimately, the variance seen in the properly aligned case, at its worst of 0.28°, is roughly 7% of the typical ASM NZ ROM in axial rotation (~4° on average). It should also be noted that the proper alignment positions are not necessarily the lowest possible variance. PRL manufactures the potted specimens within a tolerance, and deviations from the specified positioning are possible; the variance seen across the properly aligned cases is indicative of this.

In comparison to the professionally manufactured and potted vertebrae produced by PRL, human cadaver specimens must be potted by the researcher, and as such, will have a much higher potential of specimen alignment variance. Attempts have been made to set forth standards in cadaver specimen preparation to help produce more comparable test results [33], however little on specific variance has been discussed.

Control over the variance seen in the ASM potting bases is directly influenced by either adjusting the mold dimensions used to make the potting bases or machining the bases after molding. The latter would add an extra step to the manufacturing process that would add time and cost. Even with this control, it would not be feasible to size each potting base to every customer's specified dimensions. From a manufacturing standpoint, a single potting base style with tight tolerance would be the ideal format to offer. Regardless of what potting options PRL offers, it will be important to make sure that customers are aware of the presence of variance and that it is specific to their test set up.

2.5. Conclusions and Future Work

2.5.1. Conclusions

The goals of this investigation were to see if any improvements could be made on the previously developed ASM facet joint while maintaining manufacturability and its compatibility to be used with Tekscan sensors. Although the initial qualitative interface analysis was not able to make adequate comparisons across the different interface combinations, the analytical guidelines were able to be translated into qualitative guidelines that a human observer could use to make sufficient comparisons. Ultimately, it was found that although several interface

combinations were found to be acceptable and comparable to the original ASM facet interface, no single interface showed any improvement in performance and manufacturability. Each of the top interfaces produce a clearly developed TZ and showed a wide angular distance between start and end points of the TZ. Additionally, these combinations all proved to work well with Tekscan sensor use. Given these results, it is recommended that no changes need to be made to the current ASM facet joint.

The specimen potting base alignment check revealed that a certain degree of specimen performance has to be attributed to base alignment in the potting blocks and that this variance would be similar to what would be expected when working with human specimens but to a lesser degree.

2.5.2. Future Work on the ASM Facet Interface

The work presented in this report shows the development that was done to identify a joint which exhibits an adequate non-linear transition region between the NZ and EZ regions in axial rotation. Future work should investigate improvements that can be made in the other modes of bending without sacrificing the current behavior in axial rotation.

The materials included in the interface testing were identified as ones which were readily available and suitable for use in the current ASM. Future work should focus on identifying more specialized materials and furthering the development of the inverse synovial joint concept. One suggested point of interest would be to investigate the use of adding a fluid-filled bubble that could be imbedded in the surface of each articular process to allow for actual fluid to be used within the joint. Attention to how Tekscan sensors could be used with such a joint would be a critical factor to investigate.

3. Facet Joint Load Transfer

Chapter 3 presents the research conducted on the load bearing characteristics of the ASM facet joint and how it compares to human data. Background on the human facet joint and a discussion on various methods of facet load measurement are given first. The test methods used for this portion of testing are discussed, followed by the results. Several points from the results are discussed followed by conclusions and notes on future work.

3.1. Background

The following sections briefly discuss the human lumbar facet joint and the significance of it as related to research conducted on LBP. The discussion includes a brief overview of facet joint anatomy followed by a review of previous and current methods used for facet load transfer measurement. The study objectives for this experiment are also presented.

3.1.1. Human Lumbar Facet Joint

A facet joint (also called the zygapophysial or apophyseal joint) is comprised of the inferior and superior articular processes of two adjacent vertebrae. Each FSU contains two opposing facet joints. A posterior view of the facets on the ASM is shown in Figure 26.

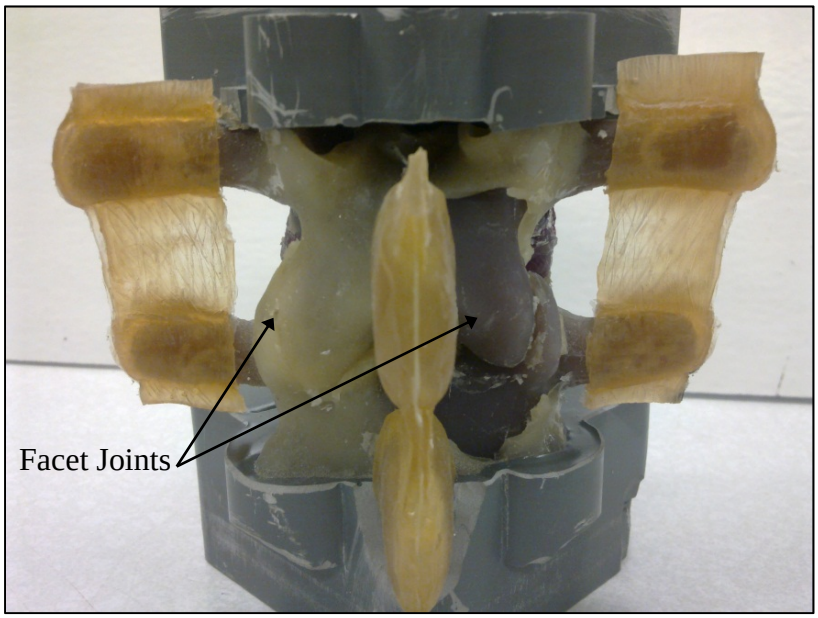

Figure 26: Posterior view of the facet joints on the analogue spine model. The right capsular ligament was removed to reveal the articular processes of the right facet joint.

The facet joint and the IVD make up the primary load transfer points in the spine. The facet joint provides three main functions within the spine:

- Transfer loads (primarily bending) across adjacent vertebrae
- Provide a means of shock absorption to dissipate peak loads
- Prevent bone-on-bone contact

The interface within the human facet joint is comprised of a layer of articular cartilage on the face of each articular process, a synovial cavity between the faces, and the capsular ligament (CL) that retains the synovial fluid in the joint as shown in Figure 27.

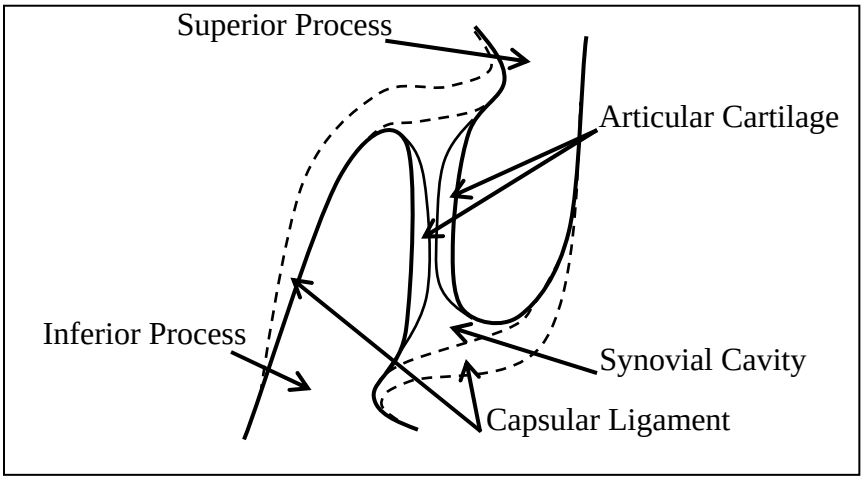

Figure 27: Diagram of the human facet joint interface. Articular cartilage coats the face of each articular process. The capsular ligaments enclose the joint and retain synovial fluid between the articular process faces.

The cartilage provides a stiff and smooth surface for load transfer. The motion is lubricated by the synovial fluid which is held within the joint by the surrounding CL.

3.1.2. Significance of Facet Load Measurement

Of the various causes of LBP, the lumbar facet joint is attributed to up to 45% of all cases [10]. With occurrence rates at nearly half of the total LBP cases, there is clearly a need to focus research on addressing LBP associated with facet joint issues. There is surprisingly little data available concerning the quantitative determination of facet behavior under axial rotation and lateral bending [34]. Additional information on the load-bearing characteristics of the facet joint would provide valuable knowledge about facet instability and degeneration [6].

3.1.3. Methods of Facet Load Measurement

There has been a large amount of research previously conducted on methods of facet load measurement of human cadaver spines. Table 6 provides a brief overview of various methods that have been proposed for facet load measurement.

Table 6: Comparison of previous and current facet load measurement techniques.

Researcher	Method	Materials	Load Measurement
Buttermann et al., 2001 [35]	Articular process strain measurement	Strain gages	Magnitude and distribution
El-Bohy et al., 1989 [36]	Direct facet pressure measurement	Needle transducer	Pressure magnitude
Hedman et al., 1997 [37]	Direct load measurement	Pressure sensitive film	Magnitude and distribution
Wilson et al., 2006 [32]	Direct load measurement	Tekscan pressure sensor	Magnitude and distribution

Each of the methods presented above attempt to either directly or indirectly measure loads or pressures developed within the facet joint. All of the methods are considered acceptable methods of facet load measurement and have been proven to provide useful results. The details of each of these methods and their relevance to the ASM are described in further detail below.

- Articular Strain Measurement: Butterman et al. have conducted extensive research on a method of facet load measurement using strain gauges applied to the bases of the articular processes [35]. A series of four strain gages are applied to a prepared articular process surface opposite the joint which allows for a gradient of strain to be measured during loading. This gradient is then translated into load and location data. This method requires a large amount of specimen preparation and system calibration. This method is less than desirable when considering implementation within the ASM. The precise placement of the strain gages along with the detail calibration would create many manufacturing complications. The acquisition and analysis of the strain gage data would likely require a software program as the translation of the strain data into load data is fairly involved.
- Pressure Needle Transducer: El-Bohy et al. described a method of direct facet pressure measurement [36]. In this method a small needle pressure transducer is inserted into the body of an articular process so that the active tip of the transducer

just penetrates through the articular cartilage of the process. This method requires that a precise hole be drilled through the process with X-Ray monitoring of the placement of the hole so as not to damage the joint. Seeing as this method relies on pressure generation inside a standard synovial joint, it would not likely be suitable for the inverse synovial joint designed for the ASM facet joint. Additionally, the complication of drilling holes into the vertebrae and embedding the transducers is less than desirable.

- Pressure Sensitive Film: Hedman et al. described a method of facet load measurement by inserting a pressure sensitive film into the facet joint [37]. This method requires an incision be made in the CLs to allow for the film to be inserted into the joint. Post processing requires development and pixilation of the film to determine the load distribution. When compared to the previous facet load measurement methods presented, this method is more ideal on many levels. The fact that the sensor integration can be done after factory assembly essentially negates any manufacturing costs associated with preparing the specimen for sensor use. Alternatively, it could be possible for PRL to embed the film into the facet joints, however this would render the film (and the facet joint) unusable after a single trial as it would have to be removed for analysis.
- Tekscan Pressure Sensor: Wilson et al. researched a method of facet load measurement using Tekscan (Tekscan Inc., South Boston MA) pressure sensors [32]. This method is similar in approach to the use of pressure sensitive film in that the sensor is inserted in the facet joint, however all of the data acquisition and analysis is handled by Tekscans integrated I-Scan software. Of the various methods presented, this one was identified as the most desirable means of facet load measurement for the ASM and as such, was the method of choice for the work done in this research [31]. A primary drawback to this method is that it requires the use of an additional test system however it has already widely been used by various research labs [38-40].

It is important to note that while the methods presented above represent currently accepted means for facet load measurement, many new technologies are being researched and developed that may prove to be superior choices in the future.

3.1.4. Study Objectives

The main purpose of this portion of research was to determine whether or not the facet load transfer characteristics of the current ASM facet joint are similar to those of the human facet joint. The goal was to identify the relationship between applied moment and resulting facet load for both the ASM and human FSUs and then compare the two. Additionally, this work was intended to investigate the validity of the load transfer characteristics of the ASM facet joint when compared to human data.

3.2. Methods

A MTS Mini Bionix 858 hydraulic load frame (MTS Systems Co, Eden Prairie MN) was used to apply loads to the test specimens. The KU Spine Biomechanics Lab (SLB) MTS machine can apply loads in three modes: axial tension and compression, axial rotation (torsion), and bending in both the lateral and flexion-extension directions (depending on specimen orientation). The machine records load (force and bending moments) and displacement (distance and angle) data for each active channel at a 100Hz sample rate. Figure 28 shows a specimen loaded in the MTS machine fixtures.

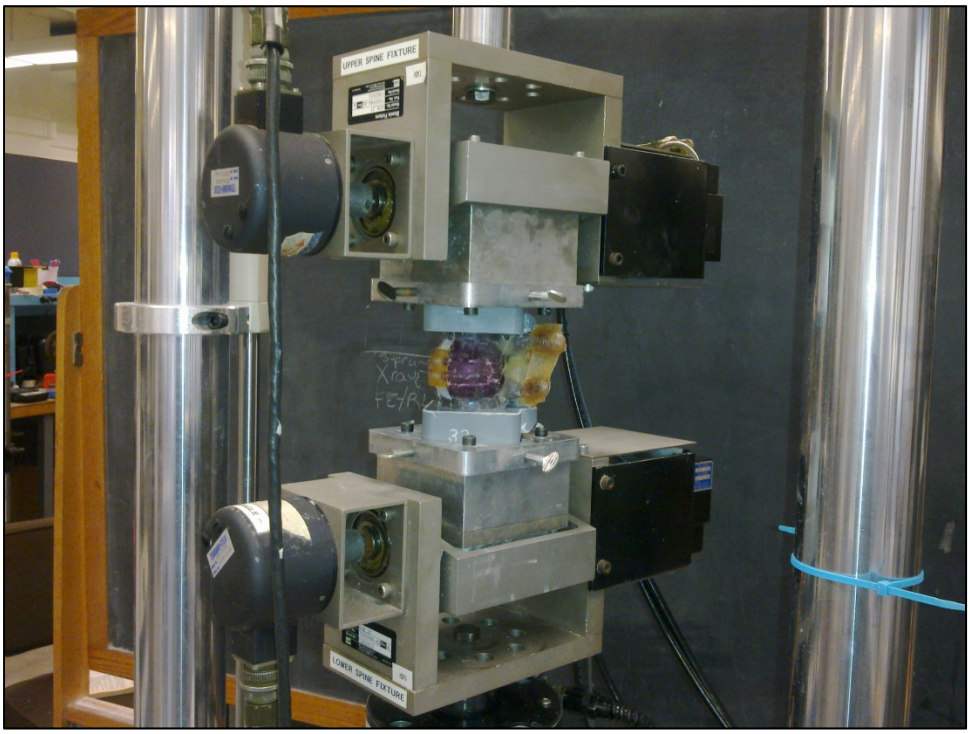

Figure 28: Functional spine unit loaded into MTS hydraulic load frame.

Lateral, flexion-extension, and axial rotation were all performed at a rate of 0.92°/sec. Wilke et al. report that any rate between 0.5°/sec and 5°/sec is reasonable and has little effect on specimen behavior [33]. An axial compressive preload is held at a constant 100N in force control throughout each test to negate pinching effects caused by the bending jigs during bending.

3.2.1. Experimental Test Equipment

A Tekscan I-Scan System was used in conjunction with Tekscan model 6900 pressure sensors to measure facet load during this experiment. The specimens were loaded in axial rotation, lateral bending, and flexion-extension using the MTS hydraulic load frame in the SBL at KU. Facet loads were measured at a sampling rate of 4Hz.

3.2.2. Specimen Preparation

This experiment included both ASM FSUs and human cadaver FSUs, each of which required different preparations. ASM FSUs are assembled and potted at PRL and then sent to KU for testing. These specimens are allowed to sit at room temperature for a minimum of 12 hours after receiving to allow any temperature differences induced during shipping to be dissipated. The specimens then undergo a break in procedure of three axial compression cycles from 0 to 2000N at 0.25cm/min followed by 100 cycles of ±1.0° of rotation in axial torsion, lateral (right-left) bending, and flexion-extension bending at a rate of 0.92°/sec.

The human specimens used in this experiment were prepared in the KU SBL. Details on each of the human specimens included in these tests can be found in Appendix B. Preparation of these specimens began by dissecting out the L3/L4 FSUs from full lumbar segments and then potting the specimens in a polyester resin. Screws were inserted into the free ends of the L3 and L4 vertebrae before submerging the free ends of the specimen to allow the polyester resin to have something to grip on to in order to provide a more rigid connection. X-rays of each specimen were taken after potting to verify that the screws were installed correctly. These specimens only saw an initial ROM test with no other break in before full load tests were conducted.

3.2.3. Experimental Test Procedure

The tests performed for this experiment were broken down into three specimen configurations: intact specimen, specimen with cut CLs, and specimen with cut CLs and Tekscan

sensor inserted. These configurations were included to monitor any change in specimen behavior that was introduced by cutting the CLs and inserting the sensors.

Before each new specimen was tested, the Tekscan sensors were equilibrated and calibrated using a single point calibration scheme with an applied compressive load of 80N using a Tekscan PB100E calibration bladder system. The single point calibration was done in accordance with work done by Wilson et al. to minimize the sensors overshoot [32]. Additionally, the single point calibration scheme is desirable because the expected load for these tests is on the low end of its full scale output (less than 10%).

For the ASM FSUs, each of the three specimen configurations includes two trials of axial rotation, lateral bending, and flexion-extension. One trial of each mode is done before running the second set of trials. Each trial includes five cycles of loading with a compressive 100N preload maintained in force control. The human FSUs were only tested for one trial to minimize the amount of time required for each test. The first specimen configuration was done with the specimen fully intact. For the second configuration, a scalpel was used to cut an incision around each facet joint to allow for sensor insertion. Care was taken to not damage the surrounding ligaments. For the third configuration, two of the four sensors on the Tekscan model 6900 sensors were inserted into the facet joints as shown in Figure 29.

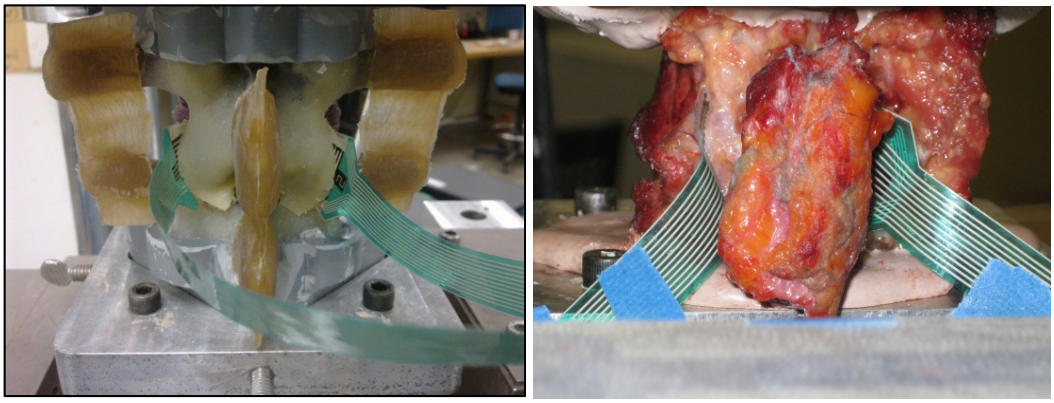

Figure 29: Tekscan sensors inserted into the facet joints of the analogue spine model (left) and a human functional spine unit (right).

When testing the ASM FSUs, a thin film of petroleum jelly was applied to each face of the sensors to allow for ease of insertion so as not to damage the sensor. This lubrication was not necessary for the human FSUs.

3.2.4. Statistical Methods

A statistical analysis was performed on the facet load data to determine the significant results. A three-way analysis of variance (ANOVA) was performed to show how facet load was sensitive to applied moment, facet side (left or right), and specimen type (ASM or human). The statistical calculations were made using IBMs SPSS software (IBM, Armonk NY).

For the specimen alignment check, paired t-tests were performed to compare the changes in stiffness made by the cutting of the CLs and the insertion of the Tekscan sensors. Two t-test were performed, one to show the significance of cutting the CLs, and the other to show the significance of inserting the sensor into the cut CLs.

3.3. Results

The Tekscan data gathered from this experiment was first processed using Tekscan's I-Scan analysis software which allows for the measurement of total force magnitude seen by a sensor over the time allotted for a test. This data was exported into Matlab along with the MTS data and processed to determine the facet loads for a specified applied moment range of ±1 to ±15Nm and ±1 to ±10Nm in 1Nm increments for ASM FSUs and human FSUs respectively. The lower range used in human FSU testing was done to avoid higher loads that could cause damage to the specimens and reduce the amount of useful data that could be obtained. The results are presented as plots showing facet load as a function of applied moment steps. The results are presented in three parts: typical ASM and human behavior, average ASM and human behavior, and an average comparison of ASM and human behavior.

Specimen stiffness values across the three specimen configurations are also presented to show the effect that cutting the CLs and inserting the Tekscan sensors has on specimen behavior.

3.3.1. Statistical Significance of Facet Load Data

The results from the three-way ANOVA are shown in Table 7. Several human specimens were not taken to the same full ROM that the ASM saw to avoid causing damage to the specimen. As such, the ANOVA was run only for the applied moment range that included all human and ASM specimens (1Nm to 5Nm).

Table 7: Results from the three-way ANOVA of the facet load data from 1Nm to 5Nm. The three dimensions of the analysis include applied moment, type (analogue spine model or human), and side (right or left facet). The statistically significant ($p<0.15$) values are highlighted in bold.

Effect	P Value
Moment	**0.002**
Moment * Type	**0.002**
Moment * Side	0.205
Side	**0.006**
Side * Type	**0.057**
Moment * Side * Type	0.232

As Table 7 shows, facet load varies significantly with applied moment, applied moment crossed with type, side, and side crossed with type.

3.3.2. Typical Facet Loads from Tekscan Data

A representative example of ASM and human facet load data as a function of applied moment is shown in Figure 30.

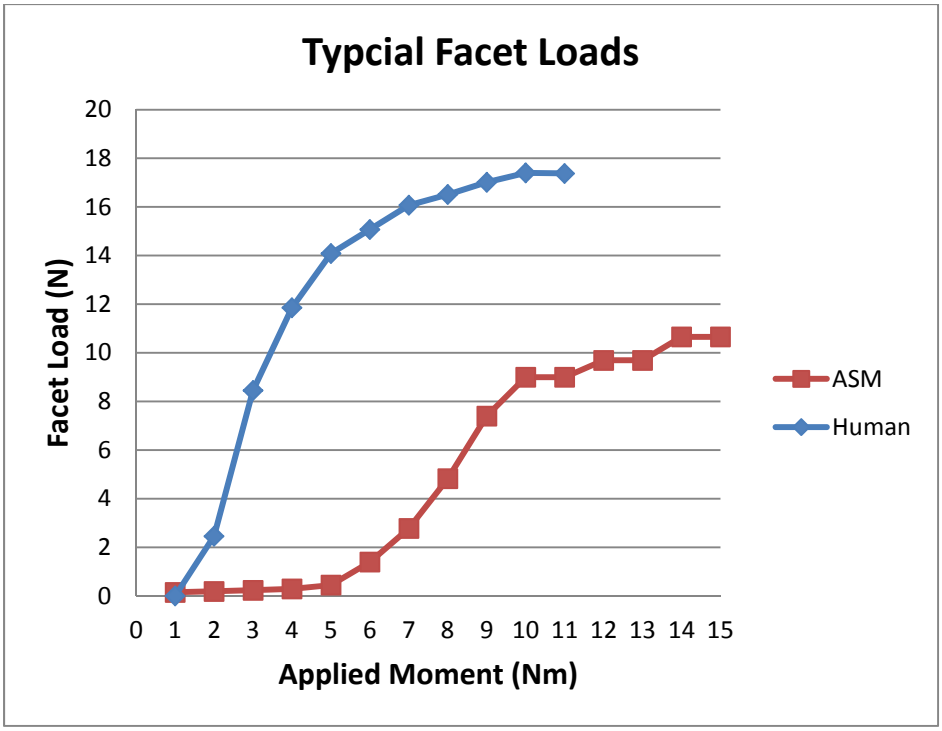

Figure 30: Example of typical facet load behavior at applied moments for the analogue spine model and human facet joints. The facet loads were determined at fixed applied moment increments of 1Nm. The analogue spine model data goes from 1Nm to 15Nm however the human data only goes up to 11Nm as a lower range of motion was used for this particular specimen to avoid damaging the specimen.

In the ASM data, there is a very slow buildup of load until approximately ±5Nm where the slope gets much steeper until it reaches a level where the load begins to show a stair-step behavior. In the human data, the slope of the line is fairly steep from 0Nm to around ±5Nm and then begins to level off as the moments go beyond ±10N. The trend of the human data is fairly smooth and consistent with no large jumps in the data.

3.3.3. Average ASM and Human FSU Facet Loads

The average left and right facet loadings for the ASM and human facet joints are shown in Figure 31.

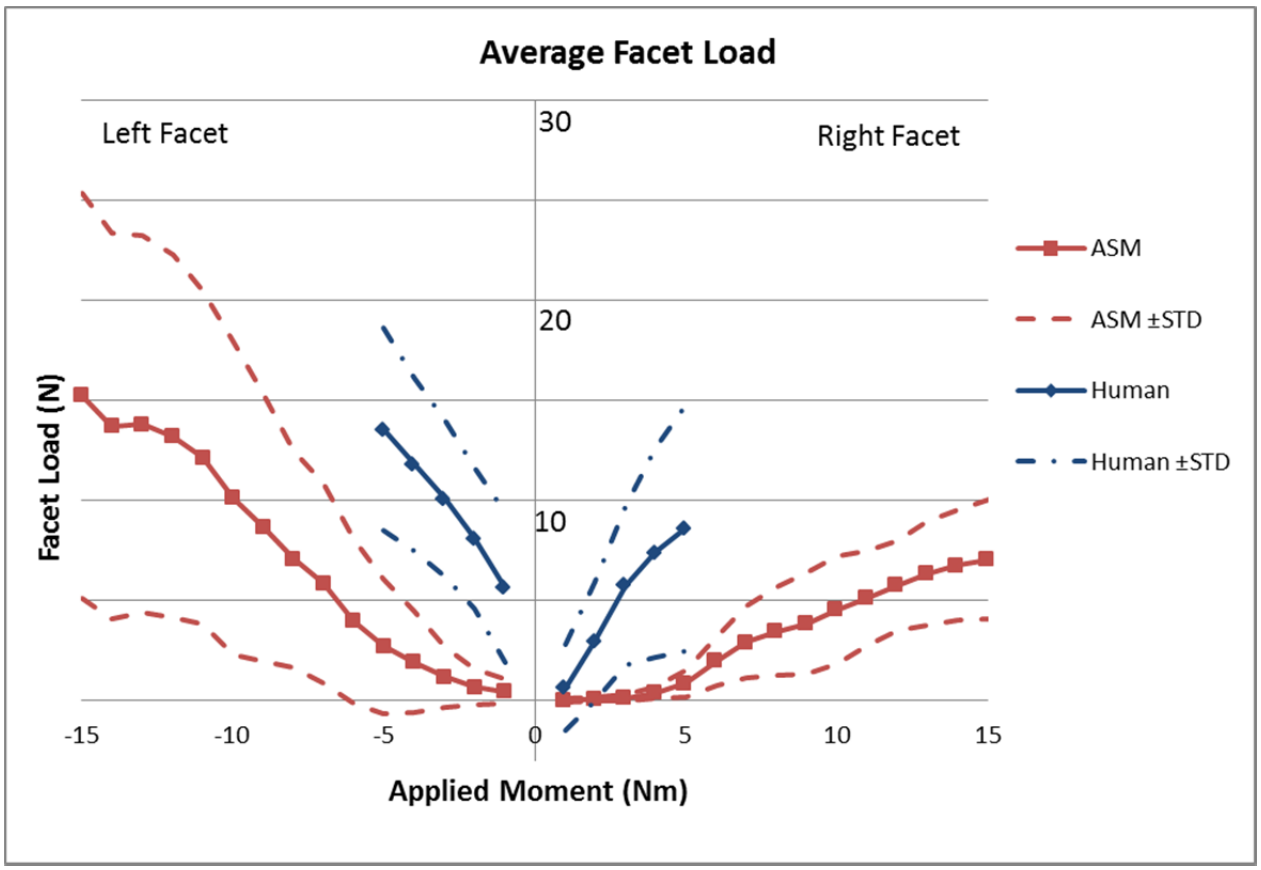

Figure 31: Average left and right facet loads for analogue spine model and human facet joints at fixed applied moment points. The human values are only shown from 1Nm to 5Nm due to limited statistical power beyond 5Nm.

3.3.4. Comparison of Average ASM and Human FSU Facet Loads

The pooled average loading (pooled right and left facets) behavior of ASM and human facet load transfer during axial rotation at fixed applied moment points from 1N to 5N are shown in Figure 32.

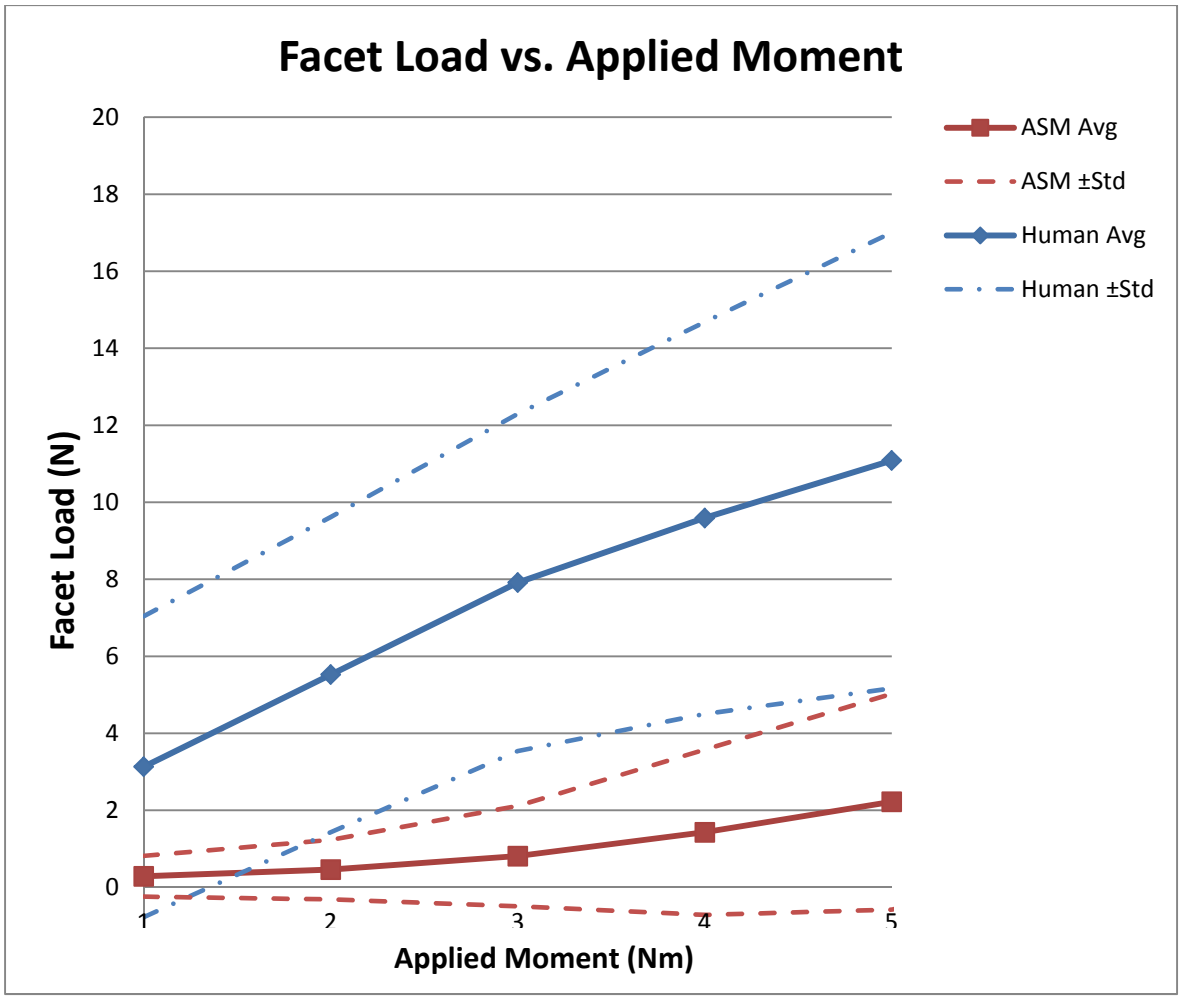

Figure 32: Comparison of average analogue spine model and human facet loads at fixed applied moment points from 1Nm to 5Nm. Standard deviations are shown as dotted lines.

3.3.5. Effect of Sensor Insertion on FSU Behavior

The NZ and EZ stiffness of axial rotation (torsion) were monitored across the three specimen configurations of this experiment, and the ASM and Human values are presented in Figure 33.

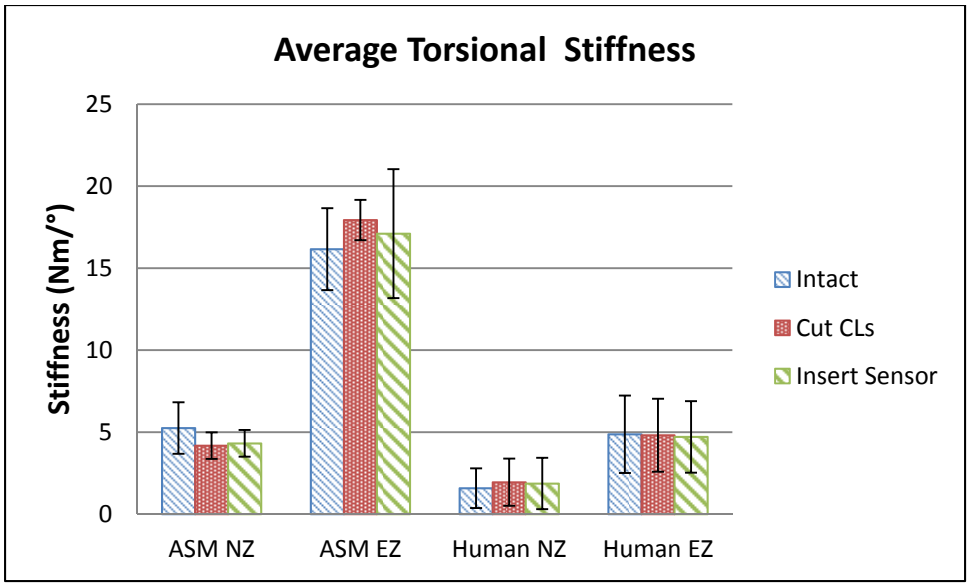

Figure 33: Change in axial rotation (torsion) stiffness across the three specimen configurations. The four data sets show the neutral zone (NZ) and extension zone (EZ) stiffness for both the analogue spine model (ASM, left two columns of data) and human specimens (right two columns of data).

Note that the largest changes in stiffness occur in the NZ region after the initial cuts are made in the CLs and that the change is less when the sensors are inserted into the facet joints. The results from the t-tests for this investigation are given in Table 8.

Table 8: P-Values from t-tests of facet load test configurations. The values reported for the Cut CLs columns are for the change made by cutting the intact capsular ligaments. The values reported for the Insert Sensor columns are for the changes seen by inserting the sensor into the joint with the cut capsular ligaments.

	Cut CLs		Insert Sensor	
	NZ	**EZ**	**NZ**	**EZ**
ASM	**0.01**	0.09	**0.03**	0.54
Human	0.10	0.56	0.43	0.21

Only The NZ stiffness showed any significant change for both configuration changes, however these were both within the standard deviations of data at these configurations. The largest change was seen when the initial incision was made in the CLs, primarily seen in the ASM results.

3.4. Discussion

3.4.1. Comparison of Human Facet Load Data to ASM Facet Load Data

As discussed in the methods section, each specimen was tested in three modes of loading. Of these three modes, it was found that axial torsion was the only one on the ASM that provided useable facet load data. Flexion-Extension data showed some load transfer, however the magnitudes were low relative to axial rotation. The data from the lateral bending were essentially null sets with hardly any load seen at all. This was mainly a result of the loading method employed by the spine bending jigs on the SBL MTS machine. The center of rotation on the MTS spine jigs is several inches above and below the anatomical centers of the L3 and L4 vertebrae respectively. For smaller angular displacements, this effect is considered small and negligible, however at larger displacements, the center of axial compression goes outside the anatomical center of the specimen (Figure 34) and the axial preload control of the MTS machine begins to induce an additional moment on the specimen which is undesirable.

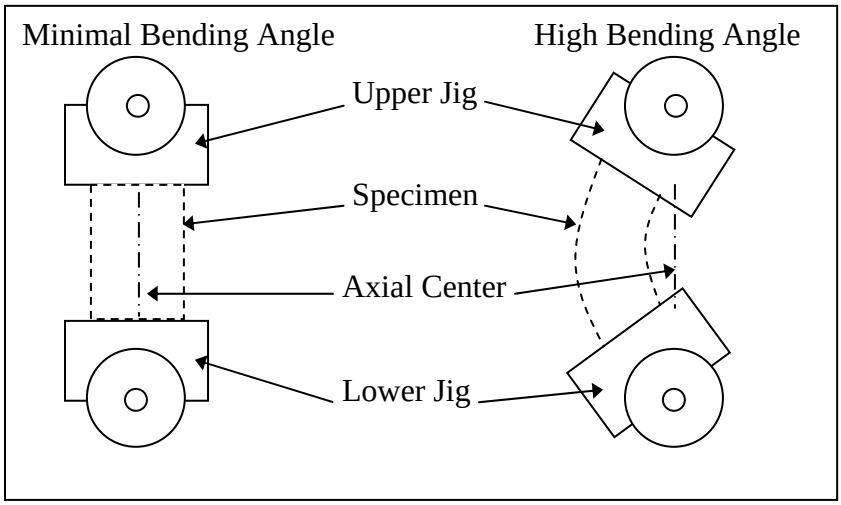

Figure 34: Offset of center of rotation on MTS bending jigs. The small circles represent the rotational axis of the bending jigs. At high bending angles the axial center goes outside of the specimen and the axial compression begins to apply an additional bending moment.

The angles at which facet contact occurs in lateral bending and flexion-extension are close to these limits and therefore these tests did not see full facet contact.

The difference seen between the average ASM and human facet load behavior is likely explained by the difference in NZ stiffness and NZ ROM between the two. The human specimens are more likely to have “realistic” spacing between facets and more contained NZ ROM which would result in a stiffer, more compact NZ. This can be seen as the facet loads rise

very rapidly in the lower ROM angles until the TZ and EZ regions are reached at which point they start to level off. The ASM specimens on the other hand are known to have a fairly wide NZ ROM [30] and have the likelihood of having a less compact distribution of facet interface materials. The behavior of the ASM appears to agree with this as it has a much lower facet loads over a wider NZ ROM until the TZ and EZ regions occur.

The results show that facet loads at corresponding applied moment points are typically lower in the ASM than in the human FSUs. This is likely another artifact of the ASM facets being slightly too wide. At lower ROM angles, there is not facet contact in the ASM, so the interface materials contribute a majority of the NZ stiffness and behavior. At corresponding ROM angles in the human data, there is likely more facet contact which results in the higher loads. This discrepancy could directly be address by the geometric adjustment of the ASM facets.

It was shown in the ANOVA results that facet load varied significantly with facet side. This may be explained by several factors. One factor might be that there are alignment issues inherent in the SBL MTS test set-up that caused the left facets to see higher loads. This issue may be a result of the actual jig alignment on the MTS machine, or it could be related to specimen alignment within the jigs as was discussed in the specimen alignment check in Chapter 2. Alternately, these results may be highlighting a physiological difference in right and left facet load which could be attributed to right or left dominance of the individual human specimens. In the ASM, there could be a similar influence due to the fact that the synthetic vertebrae were modeled after real human vertebrae which could have also had asymmetric geometry.

The ASM results appear to show a stair stepped trend at higher applied moments. These steps are likely a result of the individual ligaments and components in the model taking on load as the specimen undergoes loading. Previous work done by Domann investigated the contribution that each ligament provided to the ASMs mechanical behavior [30]. It is likely that this effect could be correlated with the results presented by Domann however that is beyond the scope of this work and should be considered for future work.

3.4.2. Impact of Cutting CLs and Inserting Sensors

As the results from the specimen stiffness check illustrate, the insertion of the sensor into the facet joint has minimal effect (no statistically significant changes) on overall axial rotational

stiffness. The changes in stiffness across each part are all within the standard deviations of each change. This implies that, as expected, the use of the Tekscan sensors does not contribute any significant change in specimen behavior when used to measure facet loads in axial rotation.

The most significant change in specimen behavior is seen when the CLs are cut in preparation for sensor insertion. In the case of the ASM FSUs, a decrease in NZ stiffness may be explained by the fact that a large amount of the interface materials are damaged and or removed from the joint when the incisions are made. The cuts were made with a standard scalpel as this is what would likely be the instrument used by potential customers of the ASM. It may be possible to make a more precise incision that results in less damage to the facet interface however this may not be a feasible procedure to expect potential customers to perform routinely. In the case of the human FSUs, the same decrease in NZ stiffness could be expected since tissue may be damaged and removed during the incision.

3.5. Conclusions and Future Work

3.5.1. Conclusions

The work presented in Chapter 3 focused on the load-bearing characteristics of the ASM facet joint. Through the use of Tekscan pressure sensors the first look at facet load behavior of the ASM was revealed. Although the ASM and human facet joints were not found to be statistically similar, the overall behavior of the ASM joint was promising and showed similar behavior to the human joint at higher applied moments. The difference in behavior was able to be explained by the understanding of the current ASM FSU.

The characteristic behavior seen across all ASM specimens provided new insight into the overall behavior of the ASM FSU. The stair stepped behavior seen at higher applied moments revealed new characteristics of the individual components that make up the ASM.

3.5.2. Future Work on ASM Facet Load Measurement

The method of specimen preparation for Tekscan sensor insertion could be developed into a standard that would allow for higher levels of consistency across ASM use. This standard could specify the method of specimen preparation including the technique used to cut the facet joint to allow for sensor insertion. A method of maintaining sensor position and alignment relative to the

specimen during testing could also be developed which would allow for better tracking of kinematic load transfer data.

As it was discussed previously, axial rotation produced the most useful results out of the three modes considered, mainly due to the fact that the facet geometry for the ASM is slightly wider and more spaced apart than a typical human specimen. These modes could be investigated at higher angular displacements however a different test apparatus or loading method would need to be utilized to achieve this.

A future study could be design to further investigate the differences in left and right facet loads. Such a test could include a larger sample size that tracks the left and right dominance of each human specimen. The tests could also be performed across different test set-ups to remove any doubt about inherent alignment issues within each.

The stair stepped behavior in facet load seen at higher applied moments could be paired with previous work done by Domann [30] to develop a new experimental procedure to determine the effect that each individual ligament has on facet load behavior. This would provide a much higher level of insight into the overall behavior of the ASM, and could be used as a tool to provide further behavioral refinements.

The current method of sensor insertion could be improved upon so that the interface materials could be remain more intact and as such, the specimen stiffness could be less affected by it. In addition to continuing to improve the current facet load measurement technique with Tekscan sensors, work should also be done to continue to investigate new facet load measurement techniques. As new technologies become available, their usefulness and validity in the measurement of facet load behavior should be investigated.

4. Conclusions and Future Work

4.1. Facet Joint Interface

Chapter 2 presented the work which investigated the facet joint interface of the ASM. The goal was to see if any improvements could be made without sacrificing the current behavior and its compatibility with the use of Tekscan pressure sensors. Of the interfaces that were considered, no single one was found to provide any improvements over the current ASM facet interface. This does not imply that a better facet interface is needed, rather it has simply provided a means for justifying the current interface and laid the ground work for further interface testing to be conducted.

The investigation of specimen alignment provided an initial check of how much angular variance could be attributed to the SBL MTS set up. This not only served as a quantitative measure, but also as an example of what each user of the ASM should be aware of. Since the ASM provides a more consistent test bed than the alternative when working with human specimens, a new level of attention to detail should be considered which previously may have not been reasonable. This will not only improve the consistency of test methods, but will also provide a better baseline for comparison across different tests.

The primary target for future improvement should focus on the interfaces ability to provide a smooth, non-linear transition from NZ to EZ stiffness. The current study focused on readily available commercial products; future work could be done to design a custom material for the facet interface that exhibits the exact desired behavior. An investigation into the customer needs of the ASM facet joint should first be conducted to justify this work. Although it was not investigated in this work, the geometry of the facets and the orientation of the ASM vertebrae in the model should also be considered as contributors to the behavior of the facet interface.

4.2. Facet Joint Load-Bearing Characteristics

Chapter 3 presented the work that investigated the load-bearing characteristics of the ASM facet joint. Although the average facet loads at the fixed applied moment points were not found to be statistically similar, many important factors were identified that are in favor of validating the ASM facet joint. The ASM showed lower facet loads compared to human behavior, but this

is likely explained by the current ASM facet geometry which could be adjusted to bring the two closer to agreement. The results from this research should be used as an initial baseline for comparison by users of the first generation of the ASM.

Future work on investigating the characteristics of the ASM facet joint should focus on effect that facet geometry has on facet load, and on how the current ASM geometry could be improved to provide a more realistic behavior. This could be done in a study which parametrically varies the facet geometry (articular processes height and angle, and also pedicle length) to show what effect the spacing and alignment of the facets has on the load transfer within the joint. An initial check of this could be done using a dynamic modeling software program such as ADAMS (MSC Software Co, Santa Ana CA) which could simplify the initial geometric investigation and avoid the need to manufacture many different sized vertebrae.

Future work should also focus on investigating and testing new alternative methods of facet load measurement. Methods of interest should include embedded sensors that could be used without the need for ASM modification. This would improve the overall behavior of the model and improve the reliability of the test results. PRL should also consider developing a proprietary acquisition system that could be integrated with such an embedded sensor to provide a more robust and useful product. This system could provide metrics which the spine research community could use as a standard for comparison.

References

1. Deyo, R.A. and J.N. Weinstein, *Low Back Pain.* N Engl J Med, 2001. **344**(5): p. 363-70.

2. Hangai, M., et al., *Factors associated with lumbar intervertebral disc degeneration in the elderly.* The spine journal, 2008. **8**(5): p. 732-740.

3. *Medtech Insight: US Markets for Spinal Fusion Products*. 2005 [cited 2011 11/26]; Available from: http://www.medtechinsight.com/ReportA303.html.

4. Dagenais, S., J. Caro, and S. Haldeman, *A systematic review of low back pain cost of illness studies in the United States and internationally.* The spine journal, 2008. **8**(1): p. 8-20.

5. Martin, B.I., et al., *Expenditures and health status among adults with back and neck problems.* JAMA: the journal of the American Medical Association, 2008. **299**(6): p. 656.

6. Lorenz, M., A. Patwardhan, and R. Vanderby Jr, *Load-bearing characteristics of lumbar facets in normal and surgically altered spinal segments.* Spine, 1983. **8**(2): p. 122.

7. Kauppila, L., *Atherosclerosis and disc degeneration/low-back pain-a systematic review.* European Journal of Vascular and Endovascular Surgery, 2009. **37**(6): p. 661-670.

8. Jhawar, B.S., et al., *Cardiovascular risk factors for physician-diagnosed lumbar disc herniation.* The spine journal, 2006. **6**(6): p. 684-691.

9. van Tulder, M.W., et al., *Spinal radiographic findings and nonspecific low back pain: a systematic review of observational studies.* Spine, 1997. **22**(4): p. 427.

10. Schofferman, J. and G. Kine, *Effectiveness of repeated radiofrequency neurotomy for lumbar facet pain.* Spine, 2004. **29**(21): p. 2471.

11. Lewinnek, G.E. and C.A. Warfield, *Facet joint degeneration as a cause of low back pain.* Clinical orthopaedics and related research, 1986. **213**: p. 216.

12. Bogduk, N., A. Wilson, and W. Tynan, *The human lumbar dorsal rami.* Journal of anatomy, 1982. **134**(Pt 2): p. 383.

13. Manchikanti, L., et al., *Prevalence of lumbar facet joint pain in chronic low back pain.* Pain Physician, 1999. **2**(3): p. 59-64.

14. Turner, J.A., et al., *Patient outcomes after lumbar spinal fusions.* JAMA: the journal of the American Medical Association, 1992. **268**(7): p. 907.

15. Harrop, J.S., et al., *Lumbar adjacent segment degeneration and disease after arthrodesis and total disc arthroplasty.* Spine, 2008. **33**(15): p. 1701.

16. Khan, S.N. and A.J. Stirling, *The case against disc replacement.* Ann R Coll Surg Engl, 2007(89): p. 6-11.

17. Okawa, A., et al., *A cadaveric study on the stability of lumbar segment after partial laminotomy and facetectomy with intact posterior ligaments.* Journal of Spinal Disorders & Techniques, 1996. **9**(6): p. 518.

18. Lynch, M. and J. Taylor, *Facet joint injection for low back pain. A clinical study.* Journal of Bone and Joint Surgery-British Volume, 1986. **68**(1): p. 138.

19. Lilius, G., et al., *Lumbar facet joint syndrome. A randomised clinical trial.* Journal of Bone and Joint Surgery-British Volume, 1989. **71**(4): p. 681.

20. Özkaya, N., M. Nordin, and D. Leger, *Fundamentals of biomechanics: equilibrium, motion, and deformation*. 1999: Springer Verlag.

21. Wikipedia. *Illu vertebral column.jpg*. 11/30/2011]; Available from: http://en.wikipedia.org/wiki/File:Illu_vertebral_column.jpg.

22. Kurtz, S.M. and A.A. Edidin, *Spine technology handbook*. 2006: Academic Press.

23. Spine, O.I. *Spinal Anatomy - Overview*. [cited 2011 11/27]; Available from: http://www.oispine.com/subject.php?pn=spinal-anatomy-018.

24. Leone, A., et al., *Lumbar Intervertebral Instability: A Review1*. Radiology, 2007. **245**(1): p. 62-77.

25. White, A.A. and M.M. Panjabi, *Clinical biomechanics of the spine*. Vol. 446. 1990: Lippincott Philadelphia.

26. Sharma, M., N.A. Langrana, and J. Rodriguez, *Role of ligaments and facets in lumbar spinal stability.* Spine, 1995. **20**(8): p. 887-900.

27. Resnick, D., S. Weller, and E. Benzel, *Biomechanics of the thoracolumbar spine.* Neurosurgery Clinics of North America, 1997. **8**(4): p. 455-69.

28. Friis, E.A., et al., *Mechanical Analogue Model of the Human Lumbar Spine; Development and Evaluation*, in *Spinal implants: are we evaluating them appropriately?* 2002, ASTM STP 1431, M.N. Melkerson, S.L. Griffith, and J.S. Kirkpatrick, Eds., ASTM International: West Conshohocken, PA. p. 143-154.

29. LaPierre, L., *Control of the Mechanical Properties of the Synthetic Anterior Longitudinal Ligament and its Effect on the Mechanical Analogue Lumbar Spine Model*, in *Department of Mechanical Engineering*. 2009, University of Kansas.

30. Domann, J.P., *Development and Validation of an Analogue Lumbar Spine Model and its Integral Components*, in *Department of Bioengineering*. 2011, University of Kansas.

31. E.E., A., et al., *Synthetic Soft Tissue Characterization of the Mechanical Analogue Lumbar Spine*. 2008: Scientific poster, 2008 Design of Medical Devices Conference, Minneapolis, MN, April 15.

32. Wilson, D.C., et al., *Accuracy and repeatability of a new method for measuring facet loads in the lumbar spine.* Journal of biomechanics, 2006. **39**(2): p. 348-353.

33. Wilke, H., K. Wenger, and L. Claes, *Testing criteria for spinal implants: recommendations for the standardization of in vitro stability testing of spinal implants.* European Spine Journal, 1998. **7**(2): p. 148-154.

34. Shirazi-Adl, A., *Finite-element evaluation of contact loads on facets of an L2-L3 lumbar segment in complex loads.* Spine, 1991. **16**(5): p. 533.

35. Buttermann, G., et al., *An experimental method for measuring force on the spinal facet joint: description and application of the method.* Journal of biomechanical engineering, 1991. **113**: p. 375.

36. El-Bohy, A.A., K.H. Yang, and A.I. King, *Experimental verification of facet load transmission by direct measurement of facet lamina contact pressure.* Journal of biomechanics, 1989. **22**(8-9): p. 931-935, 937-941.

37. Hedman, T.P. and G.R. Fernie, *Mechanical response of the lumbar spine to seated postural loads.* Spine, 1997. **22**(7): p. 734.

38. Graham, M.E., et al., *Stabilization of Joint Forces of the Subtalar Complex via HyProCure Sinus Tarsi Stent.* Journal of the American Podiatric Medical Association, 2011. **101**(5): p. 390-399.

39. Brimacombe, J.M., et al., *Effect of calibration method on Tekscan sensor accuracy.* Journal of biomechanical engineering, 2009. **131**: p. 034503.

40. Zhu, Q., et al., *Can extra-articular strains be used to measure facet contact forces in the lumbar spine? An in-vitro biomechanical study.* Proceedings of the Institution of Mechanical Engineers, Part H: Journal of Engineering in Medicine, 2008. **222**(2): p. 171-184.

Appendix A: Facet Interface Test Results

Set 1, Pair 1, Baseline

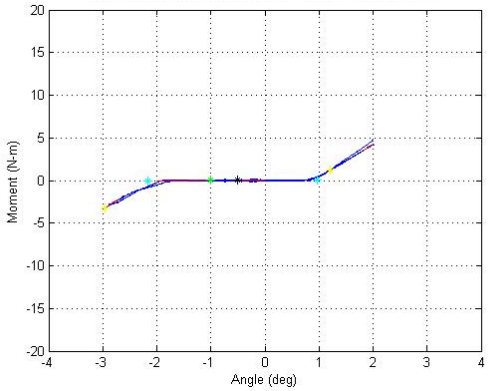

Set 1, Pair 1, A90 and Elastomer A

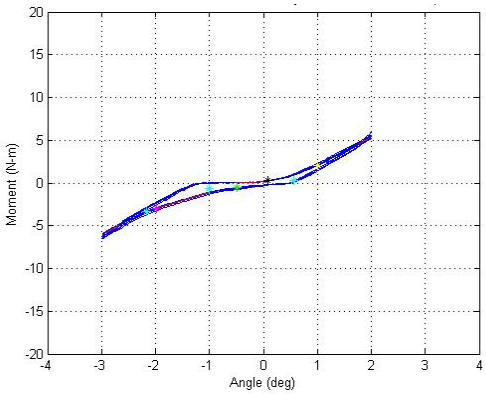

Figure 35: Performance of interface set 1, combination 1 (Paraffin and Elastomer A). The left figure shows the vertebrae test pair's baseline performance and the right figure shows the same test pair with the implemented interface.

Set 1, Pair 2, Baseline

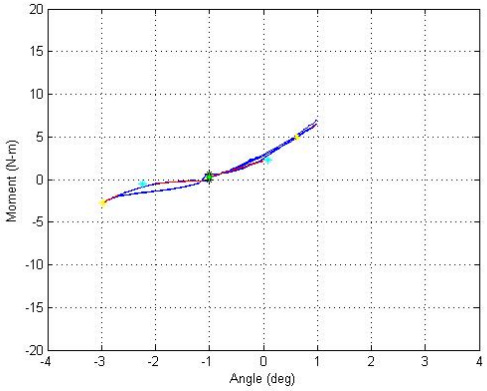

Set 1, Pair 2, A90 and Elastomer B

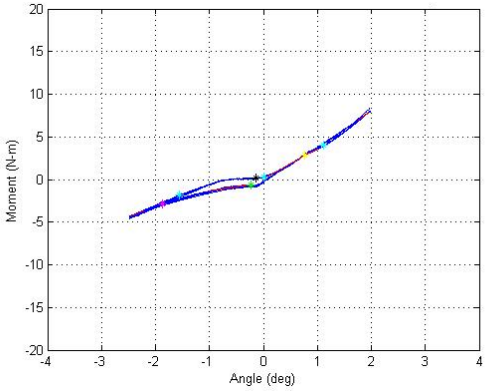

Figure 36: Performance of interface set 1, combination 2 (A90 and Elastomer B). The left figure shows the vertebrae test pair's baseline performance and the right figure shows the same test pair with the implemented interface.

Set 1, Pair 3, Baseline

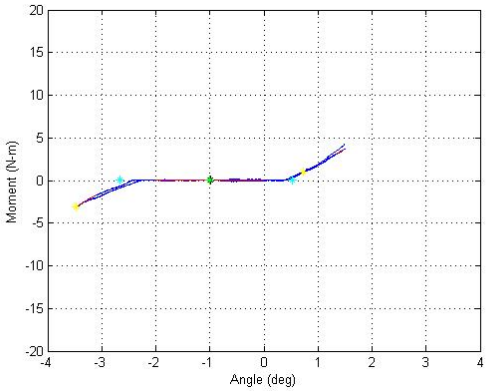

Set 1, Pair 3, Petroleum Jelly & Elastomer A

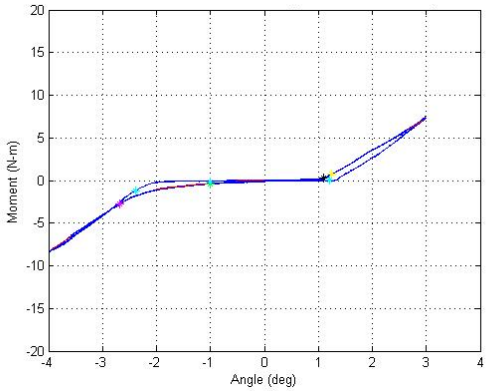

Figure 37: Performance of interface set 1, combination 3 (Petroleum Jelly and Elastomer A). The left figure shows the vertebrae test pair's baseline performance and the right figure shows the same test pair with the implemented interface.

Set 1, Pair 4, Baseline

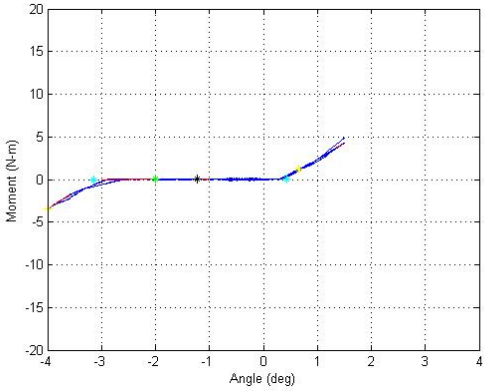

Set 1, Pair 4, Beeswax & Elastomer A

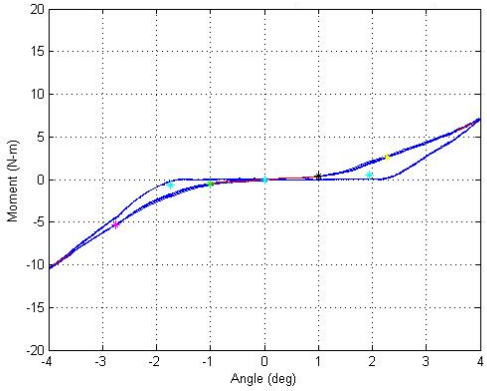

Figure 38: Performance of interface set 1, combination 4 (Beeswax and Elastomer A). The left figure shows the vertebrae test pair's baseline performance and the right figure shows the same test pair with the implemented interface.

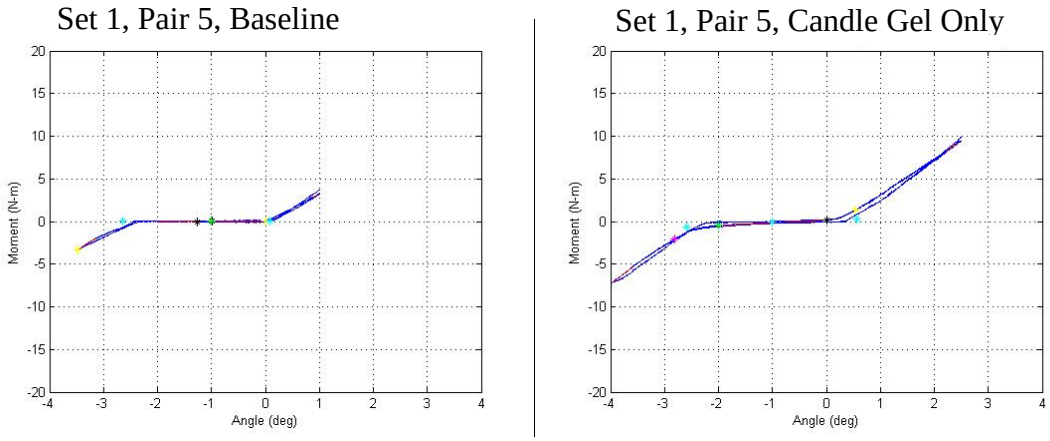

Figure 39: Performance of interface set 1, combination 5 (Candle Gel Only). The left figure shows the vertebrae test pair's baseline performance and the right figure shows the same test pair with the implemented interface.

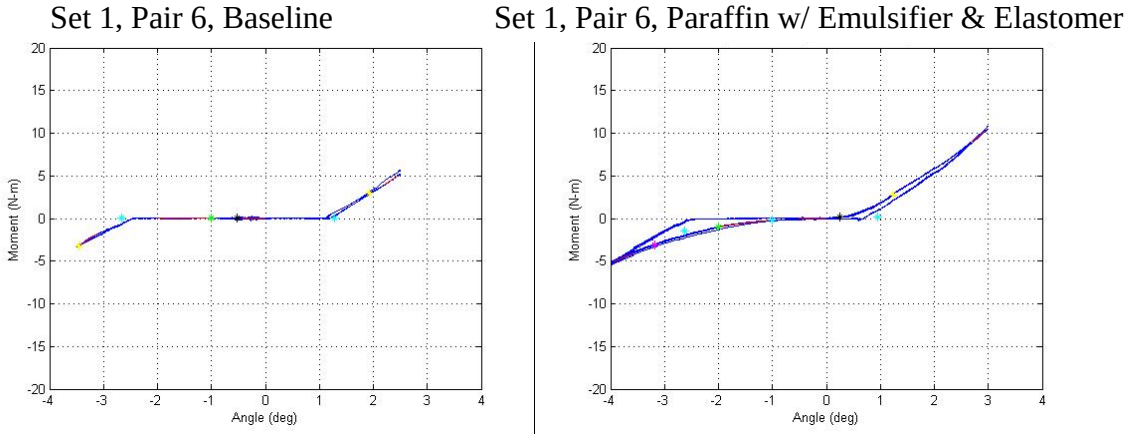

Figure 40: Performance of interface set 1, combination 6 (Paraffin with Emulsifier and Elastomer A). The left figure shows the vertebrae test pair's baseline performance and the right figure shows the same test pair with the implemented interface.

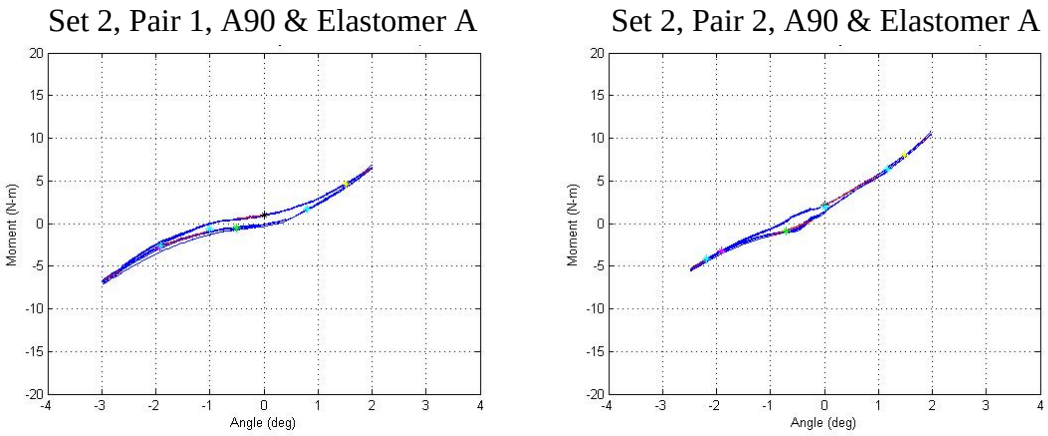

Figure 41: Performance of interface set 2, combination 1 (A90 and Elastomer A). The two figures show and compare the same interface implemented on two different specimens.

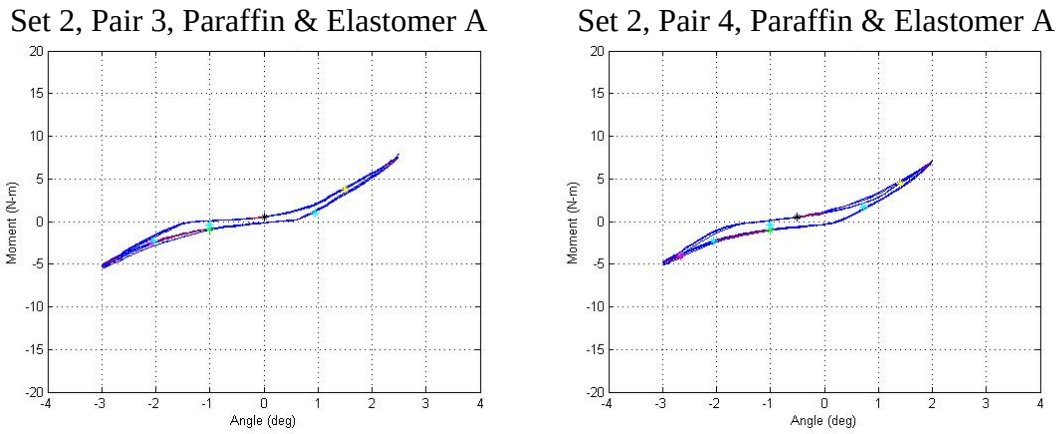

Figure 42: Performance of interface set 2, combination 2 (Paraffin and Elastomer A). The two figures show and compare the same interface implemented on two different specimens.

Set 2, Pair 5, Beeswax & Elastomer A

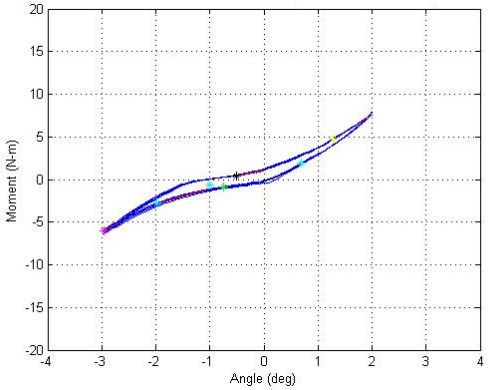

Set 2, Pair 6, Beeswax & Elastomer A

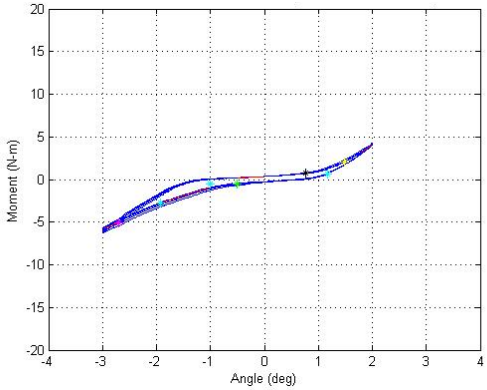

Figure 43: Performance of interface set 2, combination 3 (Beeswax and Elastomer A). The two figures show and compare the same interface implemented on two different specimens.

Appendix B: Human Specimen Information

Table 9: Specimen information for facet load tests.

Specimen	Age	Gender	Height (in)	Weight (lb)
1	-	-	-	-
2	65	M	74	236
3	38	M	71	371
4	57	F	66	200
5	63	M	74	160